IN-14292

NASA Technical Memorandum 87761

(NASA-TM-87761) MULTIGRID METHODS IN STRUCTURAL MECHANICS (NASA) 60 p
HC A04/MF A01 CSCL 20K

N86-28465

Unclas
G3/39 43401

MULTIGRID METHODS IN STRUCTURAL MECHANICS

I. S. Raju, C. A. Bigelow, S. Ta'asan and
M. Y. Hussaini

July 1986

National Aeronautics and
Space Administration

Langley Research Center
Hampton, Virginia 23665

SUMMARY

Although the application of multigrid methods to the equations of elasticity and structural mechanics has been suggested, few such applications have been reported in the literature. In the present work, multigrid techniques are applied to the finite element analysis of the deflections of a simply supported Bernoulli-Euler beam, and various aspects of the multigrid algorithm are studied and explained in detail.

In this study, six grid-fineness (or coarseness) levels, with 32 elements on the finest grid level, were used to model half the beam. To test the multigrid algorithm more severely, random initial approximations were used. With linear prolongation and sequential ordering, the multigrid algorithm yielded results which were of machine accuracy with work equivalent to 200 standard Gauss-Seidel iterations on the fine grid. Also with linear prolongation and sequential ordering, the V(1,n) cycle with n greater than 2 yielded better convergence rates than the V(n,1) cycle.

Derivation of the restriction and prolongation operators was based on energy principles. Conserving energy during the inter-grid transfers required that the prolongation operator be the transpose of the restriction operator. Maintaining an energy balance in the inter-grid transfers also led to improved convergence rates. With energy-conserving prolongation and sequential ordering, the multigrid algorithm yielded results of machine accuracy with a work equivalent to 45 standard Gauss-Seidel iterations on the fine grid. The red-black ordering of the relaxation with either linear or energy-conserving prolongation yielded solutions of machine accuracy in a single V(1,1) cycle, which required work equivalent to about 4 iterations on the finest grid level.

INTRODUCTION

Multigrid methods are known to be efficient solution techniques for certain classes of partial differential equations, and their advantages in the field of fluid dynamics have been clearly established [1,2]. Although their application to the equations of elasticity and structural mechanics has been suggested, there have been few attempts to implement multigrid methods in these cases.

Certain basic ideas underlying multigrid methods can be found in the work of Southwell [3]. However, the work of Fedorenko [4] should be regarded as the forerunner of the multigrid methods. Fedorenko solved the elliptic difference equations, using concepts of error smoothing by Jacobi relaxation and calculation of corrections on coarser grids. He also obtained an asymptotic estimate of the computational complexity for the Poisson equation on a rectangle. Fedorenko's technique was generalized by Bakhvalov [5] to include the advection diffusion equation. At about the same time, Wachpress [6] proposed a two-grid method for elliptic systems. However, multigrid methods remained virtually unused for almost a decade until the pioneering work of Brandt [7], Nicolaides [8] and Hackbush [9] revived them in the mid-1970's. Specifically, Brandt's early work established the actual efficiency of multigrid methods, and demonstrated the capability of these methods to treat nonlinear equations, general domains, local grid refinements, and solution adaptivity. He demonstrated that the maximum number of computer operations required to solve a discrete system of n equations in a Poisson problem was on the order of n computer operations. Brandt also showed how a local Fourier analysis could be used for the theoretical investigation of smoothing rates and optimization of procedures. The work of Nicolaides [8] is

the first systematic study of multigrid procedures relating to the finite element discretization of elliptic equations. A complete historical background of multigrid methods may be found in Stuben and Trottenburg [10], and Hackbush [11].

Initially, multigrid methods were successfully applied to elliptic equations to which they are particularly well suited. Recently, their use has been extended to parabolic [12] and hyperbolic [2] equations as well. Developments in multigrid methods since the mid-1970's can be found in proceedings edited by Hackbush and Trottenburg [13], Paddon and Holstein [14], and McCormick and Trottenburg [15].

Many problems in elasticity and structural mechanics are governed by elliptic equations; hence, it is quite surprising that their use in these fields remains largely unexplored. The present work is an attempt to introduce these methods to elasticians and computational structural mechanicists who have had little or no exposure to multigrid techniques. The focus of the present work is on a simple, one-dimensional example of a Bernoulli-Euler beam for the following reasons: it is amenable to local Fourier analysis, yielding smoothing and convergence factors which give an idea of the efficiency to strive for; it permits the derivation and description of various multigrid elements without the complications of higher dimensions; and it serves as a building block for implementing the algorithm in higher dimensions.

Specifically, this paper describes the finite element discretization of the relevant beam equations and discusses the performance of the Gauss-Seidel iterative technique for the solution of the resulting linear system of equations. A particular geometric multigrid scheme for accelerating the convergence (usually called the correction scheme) is presented. A general

procedure for defining the fine-to-coarse transfer of residuals (referred to as restriction) and coarse-to-fine transfer of corrections (referred to as prolongation) is described from a physical view-point. A discussion of storage and work requirements is also included.

The convergence characteristics of the solution and the number of floating point operations (work) necessary to achieve convergence are presented. Results are given for two different orderings of the iterations and for two different prolongation schemes. The effect of varying the number of iterations at each grid level is also studied.

NOMENCLATURE

A_j	Fourier series coefficients, (j = 1 to N)
b_k	element length on level k, (k = 1 to M)
B	semi-bandwidth of stiffness matrix
EI	flexural rigidity
d_j	value of direct solution at node j, (j = 1 to N_e + 1)
e	error in iterative approximation
e_m	accuracy of the machine
e_{w_i}, e_{θ_i}	error in w and θ solutions at node i, (i = 1 to N_e + 1)
$\bar{e}$	error normalized by maximum displacement
F	force vector
f_m	m^{th} component of F
h	element length on finest level
K	structural stiffness matrix
[k]	element stiffness matrix
k_{mj}	entry in m^{th} column, j^{th} row of matrix K
L	half-length of beam

M	total number of grid levels
M_0	concentrated applied moment
M_j	nodal moments
N	number of degrees of freedom
N_e	number of elements
N_i	shape functions, (i = 1 to 4)
n_1	number of iterations performed on the downward or first leg of the V-cycle
n_2	number of iterations performed on the upward or second leg of the V-cycle
P	prolongation matrix
P_0	concentrated applied force
q_0	maximum value of q(x)
$q(x)$	loading function applied to beam, $(0 \leq x \leq L)$
R	restriction matrix
R_j	nodal forces
r_i	i^{th} component of the residual vector
r_{w_j}, r_{θ_j}	w and θ residuals at node j, $(j = 1 \text{ to } N_e + 1)$
$\|\|r\|\|_2$	L_2-norm of the residuals
U	solution vector
u_i	i^{th} component of U
V	approximation to solution vector U
v_i	i^{th} component of V
W_M	work done by concentrated moment
W_n	work done by nodal forces
W_P	work done by concentrated force
w	displacement
α	arbitrary constants in displacement function

θ rotation

π strain energy

Superscripts:

f, c fine and coarse grid functions, respectively

s iteration cycle

T transpose of a matrix or vector

FORMULATION OF THE PROBLEM

One-Dimensional Beam Problem

Consider a simply supported beam of length 2L subjected to the distributed loading q(x), as shown in Figure 1. Since the problem is symmetric about the center of the beam, only one half of the beam needs to be considered. Moment equilibrium requires that

$$EI \frac{d^2w}{dx^2} = q_0 Lx \left(\frac{1}{2} - \frac{x^2}{6L^2} \right) \qquad 0 \le x \le L \qquad (1)$$

where EI is the flexural rigidity of the beam and q_0 is the maximum value of the loading function at the center of the beam.

The boundary conditions for the simply supported beam are $w(0) = w(2L) = 0$.

The exact solution for the loading shown in Figure 1 is

$$w(x) = \frac{q_0 x L^3}{120EI} \left\{ \left(\frac{x}{L}\right)^4 - 10 \left(\frac{x}{L}\right)^2 + 25 \right\} \qquad 0 \le x \le L \qquad (2)$$

To solve the problem using the finite element method, the structure is idealized by a number of beam elements. For the two-noded beam element, the displacement w and rotation dw/dx (= θ) are used as the nodal parameters. The

relevant boundary conditions are $w(0) = 0$ and $\theta(L) = 0$. The element stiffness matrix [k], obtained from the shape functions given in Appendix A, for a beam element of length b is given below.

$$[k] = EI \begin{bmatrix} 12/b^3 & 6/b^2 & -12/b^3 & 6/b^2 \\ 6/b^2 & 4/b & -6/b^2 & 2/b \\ -12/b^3 & -6/b^2 & 12/b^3 & -6/b^2 \\ 6/b^2 & 2/b & -6/b^2 & 4/b \end{bmatrix} \tag{3}$$

The element stiffness matrices are assembled into a structural stiffness matrix K and, for any given loading and boundary conditions, the system to be solved can be expressed in matrix form as the following equation:

$$KU = F \tag{4}$$

where K is a positive-definite, symmetric, square matrix, F is the load vector, and U is the vector of unknown nodal displacements and rotations.

Conventional finite element analyses typically use direct solution techniques, such as Gaussian elimination or Cholesky decomposition, to solve equation (4). With increasing discretization, solution time can become critical; thus, an attractive alternative to a direct solution is an efficient iterative technique.

Iterative Solution Techniques

Two widely used iterative solution techniques are Jacobi iteration and Gauss-Seidel iteration. The Gauss-Seidel method is used in the present work.

Gauss-Seidel Iteration

Starting with U^1 as the initial approximation to the vector of unknowns U, Gauss-Seidel iteration uses the following algorithm to calculate u_m^{s+1}, the m^{th} component of U:

$$u_m^{s+1} = \frac{1}{k_{mm}} \left[f_m - \sum_{j=1}^{m-1} k_{mj} u_j^{s+1} - \sum_{j=m+1}^{N} k_{mj} u_j^{s} \right] \quad (m = 1,2,\ldots,N) \qquad (5)$$

where u_m^s and f_m are the m^{th} components of U and F, and s indicates the iteration number. The iteration is continued until the required number of iterations has been completed or until the change in the current estimate of the solution vector is less than some given tolerance.

Convergence Study

To study the convergence of the Gauss-Seidel method, the beam problem shown in Figure 1, with one half the beam modeled with 32 elements, was considered. The convergence of the Gauss-Seidel iteration was monitored by calculating the L_2-norm of the residuals, denoted as $||r||_2$. In discrete form, assuming all elements are of equal length b, the L_2-norm can be expressed as follows:

$$||r||_2 = \sqrt{\frac{b}{L} \sum_{i=1}^{N} r_i^2} \qquad (6)$$

where the residual r_i is defined as follows:

$$r_i = f_i - \sum_{j=1}^{N} k_{ij} u_j \qquad (i = 1 \text{ to } N) \qquad (7)$$

In the present finite element context, the residuals in each equation can be thought of as the unbalanced forces and moments. So that all the residuals will have the same dimensions, the moment residuals were normalized by b, the element length. A non-dimensional L_2-norm can then be computed as follows:

$$||r||_2 = \sqrt{\frac{b}{L}\left[\sum_{i=1}^{N_e}\left\{r_{w_i}^2(x) + [r_{\theta_i}(x)/b]^2\right\}\right]/(q_0 L)} \qquad (8)$$

where r_w and r_θ are the w and θ residuals. The L_2-norm has also been divided by the factor $q_0 L$ (the total load on the beam) to produce a dimensionless quantity.

To start the Gauss-Seidel iteration, a random initial approximation for U was chosen. Figure 2 shows the L_2-norm plotted versus the number of iterations for two procedures. In the first procedure, the iterations were performed sequentially from node 1 (at the support) to node 33 (at the center of the beam). These results are shown by the solid line in Figure 2. In the other procedure, the so-called red-black ordering was used. In this ordering, all the even-numbered nodes are designated red and all the odd-numbered nodes are designated black. Iterations are performed on all the red nodes first, then the black nodes. The results of the red-black ordering are shown by the dashed line in Figure 2. For both methods, the L_2-norm drops rapidly in the first 50 iteration cycles; thereafter, the convergence slows, although the red-black ordering produces slightly better results than the sequential ordering for large numbers of iterations. However, even after 1600 iterations, the L_2-norm for both is still quite high, indicating that the iterative solution is still grossly in error. Appendix B further examines the convergence of this problem.

This behavior is inherent in the Gauss-Seidel method, since Gauss-Seidel efficiently removes the high frequency errors but not the low frequency errors. However, the low frequency errors, since they are smooth, can be approximated on coarser levels where they become higher frequency errors. On coarser levels, these high frequency errors can then be removed more

efficiently. Even if the errors are still smooth on coarser levels, iterations on the coarser levels require much less work due to the decrease in the number of unknowns. These ideas are exploited in the multigrid procedure in a recursive manner to improve the convergence rate.

MULTIGRID PROCEDURES

In this section, the multigrid method is described. In multigrid terminology, relaxation is used to mean iterations of some smoothing technique, such as the Gauss-Seidel described above; thus, to perform relaxations on a set of equations means to iterate using a smoothing method. Often, the terms relaxation and iteration are used interchangeably in multigrid literature. In the remainder of this paper, the term relaxation is used to mean Gauss-Seidel iteration, and n relaxations means n iterations on the system of equations.

The multigrid techniques are iterative methods that use a sequence of grids and a simple relaxation scheme such as Gauss-Seidel. As previously stated, such relaxation is very efficient for removing the high frequency errors on a given grid. The remaining low frequency errors become higher frequency errors on coarser grids, where they can be effectively smoothed. The key elements of the multigrid procedure are the relaxation technique and the coarse grid correction. The multigrid algorithm described here is generally called a geometric multigrid method.

Coarse Grid Correction

Consider the interplay between a coarse grid and a fine grid, where the coarse grid has half as many node points as the fine grid. Let the following equation be the discrete finite element representation of the given problem on a fine grid.

$$K^f U^f = F^f \tag{9}$$

If V^f is the approximation obtained on the fine grid after a few relaxation sweeps, then the error $e^f = U^f - V^f$ satisfies the following equation:

$$K^f e^f = r^f \tag{10}$$

where r^f, the residual on the fine grid, is defined as $r^f = F^f - K^f V^f$.

If e^f is a smooth function, e^f can be approximated by a coarse grid function e^c which satisfies the following equation:

$$K^c e^c = r^c \tag{11}$$

where $r^c = \mathbf{R}\,(r^f) = \mathbf{R}\,(F^f - K^f V^f)$

Here **R** is the fine to coarse grid restriction operator. Since the coarse grid has half as many grid points as the fine grid, it is more economical to solve equation (11) than (10). After solving equation (11) approximately by some method, the approximate error e^c is used to accelerate convergence of the fine grid solution using the following:

$$V^f \leftarrow V^f + P(e^c) \tag{12}$$

Here **P** is the prolongation operator that interpolates from the coarse grid to the fine grid and the arrow $\leftarrow$ means that the left side is replaced by the right side.

The process of calculating r^c, solving for e^c, and interpolating the results to the fine grid is called the coarse grid correction. To solve equation (9) efficiently, the above procedure is applied recursively using multiple grids. This recursive procedure is described in the following section.

Multigrid Cycle

Figure 3 shows the sequence of grid levels, k = 1 to M, for a simply supported beam where the element size b_k satisfies the relation $b_k = 2^{k-1}h$ and

h is the element size on the finest grid level (k =1). The equation on level k is written as follows:

$$K^k U^k = F^k \tag{13}$$

For k = 1 (the finest level), $K^1 = K$ and $F^1 = F$, respectively the given stiffness matrix and right-hand side of the original problem. The basic algorithm must determine the solution of the algebraic system in equation (13) on the finest grid, k = 1. The fundamental idea is to use the solutions from the progressively coarser grid levels to construct other finite element solutions in the form of equation (13). This procedure is called smoothing; in practice, it is carried out by means of relaxation. A commonly used technique is the Gauss-Seidel method.

Starting on the finest level, k = 1, let V^1 be an approximation to U^1 in equation (13), and define the residual on the finest level as $r^1 = F^1 - K^1 V^1$. If e^1 denotes the error $U^1 - V^1$, the error and the residual are related through the following equation:

$$K^1 e^1 = r^1 \tag{14}$$

For all subsequent levels (k > 1), the residual r^k is the restriction of the residual from the previous level k - 1 defined by the following equation:

$$r^k = R\,(r^{k-1} - K^{k-1} e^{k-1}) \tag{15}$$

and, therefore, the equation to be solved is now the error equation:

$$K^k e^k = r^k \tag{16}$$

Given an approximate solution V^k to the equation (13), the multigrid cycle for improving this approximation can be executed recursively as follows.

If k = 1, perform n_1 relaxation sweeps on equation (13), thereby obtaining an approximate solution V^1. Calculate the residual $r^1 = F^1 - K^1 V^1$.

Down-Sweep:

For $1 < k < M$, repeat steps (1) and (2); for $k = M$, go to step (3), with these steps defined as follows:

(1) On the current level k, start with an initial approximation $e^k = 0$, and perform n_1 relaxation sweeps on equation (16), obtaining a new approximation e^k.

(2) Restrict the residual to the next coarser level, $k + 1$, where $r^{k+1} = R(r^k - K^k e^k)$, and set $k = k + 1$.

(3) If $k = M$, solve equation (16) exactly, set $k = M - 1$, and start the up-sweep.

Up-Sweep:

For $M > k > 1$, repeat steps (4) and (5); when $k = 1$, go to step (6), where these steps are defined as follows:

(4) Update the approximation to the error e^k on the current level by adding the prolongated correction of the error from the previous coarser level:

$$e^k \leftarrow e^k + P(e^{k+1}) \tag{17}$$

(5) Perform n_2 relaxations on equation (16), starting with the updated error e^k from equation (17). This will result in an improved approximation to e^k. Set $k = k - 1$.

(6) For $k = 1$, calculate an updated approximation to the solution $V^1 \leftarrow V^1 + P(e^2)$, and perform n_2 relaxations on equation (14), obtaining an improved approximation to V^1.

The cycle described above in steps (1) through (6) is called a V-cycle, indicated by the notation $V(n_1,n_2)$, where n_1 indicates the number of relaxation sweeps performed at each level on the first or downward leg of the V-cycle and n_2 indicates the number of relaxation sweeps performed at each

level on the second or upward leg of the cycle. Figure 4 shows a schematic drawing of a V-cycle for six grid levels. A flowchart for one V-cycle is shown in Figure 5.

Restriction and Prolongation Matrices

From the foregoing description of the correction scheme, it is apparent that the keys to the multigrid procedure are the restriction and prolongation operators. These operators are related to each other as explained below.

From equations (16), the residual relations on the coarse and fine grid are written as follows:

$$K^c e^c = r^c \qquad\qquad K^f e^f = r^f \tag{18}$$

If e^f is smooth, it can be represented on a coarser level. In that case, the coarse and fine grid errors can be related using the prolongation operator P in the following equation:

$$e^f = Pe^c \tag{19}$$

and the residuals r^f and r^c can be related through the restriction operator R as follows:

$$r^c = Rr^f \tag{20}$$

In equations (18), the errors, e^c and e^f, can be thought of as representing the displacements of the respective grids, while the residuals, r^c and r^f, can be thought of as the forces required to produce these displacements. Thus, the strain energy of the coarse and fine grids can be expressed in terms of the error equations by the following expressions:

$$\pi^c = \frac{1}{2}(e^c)^T r^c \qquad\qquad \pi^f = \frac{1}{2}(e^f)^T r^f \tag{21}$$

From equations (18), (19) and (20), the strain energies of the coarse and fine grids may be rewritten as follows:

$$\pi^c = \frac{1}{2} (e^c)^T R\, r^f$$

$$\pi^f = \frac{1}{2} (e^c)^T P^T r^f \qquad (22)$$

If the strain energy is to remain constant during intergrid transfers, π^c must equal π^f. Thus, for arbitrary values of e^c and r^f, R must equal P^T to maintain an energy equivalence between grid levels.

One-Dimensional Beam Example

Before applying the multigrid cycle to the solution of the beam problem, the restriction matrix R and the prolongation matrix P must be defined.

Restriction Matrix

The restriction matrix R is defined to transfer the loads and moments from a fine grid to a coarse grid. To form this matrix, the consistent load relations must be formulated for transferring the loads and the moments. With equations (A2) and (A3), it is possible to determine the nodal forces in the beam element equivalent to a concentrated force and moment applied at the center of the element. The details of this formulation are given below.

Concentrated force. The nodal forces equivalent to a concentrated force P_0 applied at the center of an element of length b are found by equating the work done by the concentrated force to the work done by the unknown nodal forces.

W_P, the work done by the concentrated force, is equal to the force P_0 times the displacement of that force:

$$W_P = P_0 \times w(x=b/2) \qquad (23)$$

The substitution of x = b/2 into equations (A2) and (A3) yields the following result:

$$W_P = P_0 \times \{w_1/2 + \theta_1(b/8) + w_2/2 - \theta_2(b/8)\} \qquad (24)$$

Similarly, the work done by the nodal forces acting at the two end nodes can be written as follows:

$$W_n = R_1 w_1 + R_2 w_2 + M_1 \theta_1 + M_2 \theta_2 \tag{25}$$

where R_1, R_2 are the nodal forces and M_1, M_2 are the nodal moments.

W_P should equal W_n for any arbitrary values of w_1, w_2, θ_1, and θ_2. Thus, the consistent forces are

$$R_1 = R_2 = P_0/2$$
$$M_1 = P_0 b/8 \qquad M_2 = -M_1 \tag{26}$$

Concentrated moment. As before, the nodal forces equivalent to a concentrated moment M_0 applied at the center of the beam element are found by equating the work done by the concentrated moment to the work done by the unknown nodal forces.

W_M, the work done by the concentrated moment, is equal to the product of the moment M_0 and the rotation caused by that moment:

$$W_M = M_0 \times \theta(x=b/2) \tag{27}$$

To determine θ in an element, equation (A2) must be differentiated with respect to x, yielding the following equation:

$$\theta = \frac{dw}{dx} = w_1\left[-\frac{6x}{b^2} + \frac{6x^2}{b^3}\right] + \theta_1\left[1 - \frac{4x}{b} + \frac{3x^2}{b^2}\right]$$
$$+ w_2\left[\frac{6x}{b^2} - \frac{6x^2}{b^3}\right] + \theta_2\left[-\frac{2x}{b} + \frac{3x^2}{b^2}\right] \qquad 0 \le x \le b \tag{28}$$

Substituting $x = b/2$ into equation (28) and simplifying, the work due to the concentrated moment M can be written as follows:

$$W_M = M_0 \times [(-3/2b)w_1 - \theta_1/4 + (3/2b)w_2 - \theta_2/4] \tag{29}$$

As for the concentrated force, the work due to the nodal forces is written as follows:

$$W_n = R_1 w_1 + R_2 w_2 + M_1 \theta_1 + M_2 \theta_2 \tag{30}$$

where R_1, R_2 are the nodal forces and M_1, M_2 are the nodal moments.

Again, W_M should equal W_n for any arbitrary values of w_1, w_2, θ_1, and θ_2. Thus, the equivalent nodal forces for the case of the concentrated moment can be expressed as follows:

$$\begin{aligned} R_1 &= -3M_0/(2b) & R_2 &= -R_1 \\ M_1 &= -M_0/4 & M_2 &= M_1 \end{aligned} \tag{31}$$

Consistent residual transfer. The consistent nodal forces and moments given in equations (26) and (31) are used to determine the residual weights for use in the energy-conserving inter-grid transfer.

To form the restriction matrix using the force and moment weights, consider two grid levels as shown in Figure 6. Here the fine grid has three node points and two elements, while the coarse grid has two node points and one element. The lengths of the elements in the fine and coarse grids are b/2 and b, respectively. The restriction matrix R is defined to restrict the forces and moments from the fine grid to the coarse grid. The transfer of the forces and moments is shown in Figure 6 and defined below.

$$r^c = \mathbf{R}[r^f]$$

where

$$r^f = \{R_i \quad M_i \quad R_j \quad M_j \quad R_k \quad M_k\}^T \qquad r^c = \{R_i, M_i, R_k, M_k,\}^T$$

$$R = \begin{bmatrix} 1 & 0 & 1/2 & -3/(4b) & 0 & 0 \\ 0 & 1 & b/4 & -1/4 & 0 & 0 \\ 0 & 0 & 1/2 & 3/(4b) & 1 & 0 \\ 0 & 0 & -b/4 & -1/4 & 0 & 1 \end{bmatrix} \qquad (32)$$

This restriction matrix is valid only when the element size is doubled at each coarser grid level.

Prolongation Matrix

The prolongation matrix defines the displacements on the fine grid given the displacements on the coarse grid. To obtain this matrix, again consider the two grid levels shown in Figure 6. Here the displacements w and θ are known on the coarse grid at nodes i' and k'. From these displacements, the displacements at nodes i, j and k on the fine grid can be found in two ways. In either method, the displacements at nodes i and k of the fine grid are the same as the displacements of nodes i' and k' on the coarse grid. The displacements at node j on the fine mesh are found in two ways. One method assumes that the displacements at node j are the average of the displacements at nodes i' and k' on the coarse mesh. This amounts to linear interpolation as defined below:

$$w^c = P[w^f]$$

where

$$w^f = \{ w_i \quad \theta_i \quad w_j \quad \theta_j \quad w_k \quad \theta_k \}^T \qquad w^c = \{ w_{i'} \quad \theta_{i'} \quad w_{k'} \quad \theta_{k'} \}^T$$

$$P = \begin{bmatrix} 1 & 0 & 0 & 0 \\ 0 & 1 & 0 & 0 \\ 1/2 & 0 & 1/2 & 0 \\ 0 & 1/2 & 0 & 1/2 \\ 0 & 0 & 1 & 0 \\ 0 & 0 & 0 & 1 \end{bmatrix} \qquad (33)$$

In the other method, the element shape functions given in equations (A2) and (A3) are used for the interpolation. The displacements at the center of the element in the coarse mesh are found by substituting x = b/2 into equations (A2) and (A3). These are the displacements at node j on the fine mesh. The prolongation matrix thus obtained is given below:

$$P = \begin{bmatrix} 1 & 0 & 0 & 0 \\ 0 & 1 & 0 & 0 \\ 1/2 & b/4 & 1/2 & -b/4 \\ -3/(4b) & 1/4 & 3/(4b) & -1/4 \\ 0 & 0 & 1 & 0 \\ 0 & 0 & 0 & 1 \end{bmatrix} \tag{34}$$

The prolongation matrix obtained using the element shape functions is exactly the transpose of the restriction matrix given in equation (32). Thus, the use of this prolongation matrix maintains an energy equivalence between grid levels. Again, this prolongation matrix is valid only when the element size is doubled at each coarser grid level.

Although the restriction and prolongation operators derived here are for a one-dimensional problem, the procedure used here can be applied to two- or three-dimensional problems.

Storage and Work Requirements

The storage requirements necessary to solve the equation KU=F using direct solution techniques are easily calculated from the total number of degrees of freedom in the problem and the semi-bandwidth of the stiffness matrix K. Since the multigrid method is being proposed as an alternate solution technique, the storage requirements of the multigrid method should also be addressed.

Obviously, the multigrid method requires more storage space than direct solution techniques if all entries within the bandwidth are stored. The original stiffness matrix must be stored as the finest grid level and additional grid levels must be accommodated. If the finest grid has N_e elements, the coarser levels have $N_e/2$, $N_e/4$, ..., etc., elements. Thus, the total number of elements for M levels is

$$N_e + N_e/2 + N_e/4 + N_e/8 + \ldots + N_e/(2^{M-1}) = 2N_e(1 - \frac{1}{2^M}) < 2N_e \qquad (35)$$

The total number of degrees of freedom is computed in a similar fashion. In the present one-dimensional case, for N_e elements on the finest grid, there are (N_e+1) nodes, each with 2 degrees of freedom. Hence, the total storage required, assuming a constant semi-bandwidth B, can be found from the following expression:

$$2B(N_e+1) + 2B(\frac{N_e}{2}+1) + 2B(\frac{N_e}{4}+1) + \ldots = 2B(M +$$

$$2N_e\{1-\frac{1}{2^M}\}) < 2B(2N_e+M) \qquad (36)$$

Thus, the maximum storage required is always less than $2B(2N_e+M)$.

This computation assumes the storage of all entries within the bandwidth, which may result in the storage of several zero entries. These zero entries must be stored in direct solution techniques since during the solution phase some zero entries may become nonzeroes. Examination of the Gauss-Seidel iteration in equation (5) shows that only the nonzero terms of the matrices need to be stored. However, storing only the nonzero entries requires the

additional storage of pointer arrays for each row of the stiffness matrix. Many finite-element stiffness matrices are sparsely populated and, in such cases, the storage of only the nonzero terms, with the pointer arrays, can considerably reduce the storage requirements compared with banded or profile storage schemes.

With the definition of the coarser grids used here, the total storage required by the stiffness matrices of all levels should be less than twice that needed by the finest level. Additionally, the solution vectors for each grid must be stored, as well as the load vectors, or right-hand sides. Depending upon the structure of the problem, it may be advantageous to store the restriction and prolongation matrices as well.

The work (number of floating point operations) done in a single $V(n_1,n_2)$ cycle is equivalent to $2(n_1+ n_2)$ times the work of a single relaxation on the finest grid level. This is determined as follows. In the $V(n_1,n_2)$ cycle, $n_1+ n_2$ relaxations are done on the finest level while the total sum of the relaxations done on the lower levels is always less than or equal to $n_1+ n_2$. Because each subsequently coarser grid level has half as many degrees of freedom as the one before, the total number of degrees of freedom in all levels is always less than twice the number in the finest grid (see equation (36)). The work done iterating on each level is directly related to the number of degrees of freedom that must be relaxed. Thus, the total work done in a single $V(n_1,n_2)$ cycle is less than the work of $2(n_1+n_2)$ relaxations on the finest grid level.

RESULTS AND DISCUSSION

In this section the performance of the multigrid algorithm in solving the simply supported beam problem of Figure 1 is evaluated. Six grid levels are

used, where the finest mesh (level 1) has 32 elements modeling half the beam, the next coarser grid (level 2) has 16 elements modeling half the beam, and so on until the coarsest grid (level 6), which has one element modeling half the beam.

The two prolongation operators mentioned earlier are considered: a simple linear interpolation and a prolongation operator based on a constant energy in each grid level.

Results are presented for a $V(n_1,n_2)$ cycle. The convergence of the solution and the work necessary to achieve convergence are presented.

Convergence of the solution was monitored with the L_2-norm of the residuals, defined in equation (8). While the displacements converge to the exact solution within machine accuracy, the L_2-norm, because of its definition, converges with less accuracy than the displacements. Appendix C further explains this behavior.

Results are given first for sequential ordering with linear prolongation, for varying values of n_1 and n_2, and then with the energy-conserving prolongation. Finally, the effects of red-black ordering are presented.

Sequential Ordering

Linear Prolongation

Figure 7 presents the L_2-norm plotted against an increasing number of V-cycles for both random (solid line) and zero (dashed line) initial approximations. These results are for a V(2,1) cycle where the coarsest level was solved exactly. As seen in the figure, at the end of 20 V-cycles, the L_2-norm is on the order of 10^{-3} for the random initial approximation and on the order of 10^{-6} for the zero initial approximation, indicating that the multigrid solution is close to the direct solution obtainable on the finest grid level. The rates of convergence (indicated by the slope of the curves) are almost

identical for both the zero and random initial approximations. To test the algorithm more severely, only the random initial approximation is used in the remainder of this work. The work necessary to achieve the accuracy shown in Figure 7 is $2(n_1 + n_2)$ times 20 V-cycles, or equivalent to the work of 120 relaxations on the finest grid level.

Varying n_1 and n_2

To study the effect of varying the number of relaxations on either leg of the V-cycle, two cases with linear prolongation were considered. In the first case, the number of relaxations on the downward leg of the cycle was held constant at $n_1 = 1$, while the number of relaxations on the upward leg of the cycle was increased from 1 to 5 ($n_2 = 1$ to 5). Figure 8 shows the L_2-norm as a function of increasing n_2. As expected, the rate of convergence improves with increasing n_2. For the V(1,5) cycle, the L_2-norm is on the order of 10^{-7} after about 18 V-cycles. The work of 18 V(1,5) cycles is equivalent to that of 216 relaxations on the finest grid level.

The second case, $n_2 = 1$ while n_1 was increased from 1 to 5, is shown in Figure 9. As in the previous case, the rate of convergence improved with increasing numbers of relaxations. For the V(5,1) cycle, the L_2-norm is on the order of 10^{-6} after about 18 V-cycles, compared to 10^{-7} for the V(1,5) cycle of the previous case. As before, the work of 18 V(1,5) cycles is equivalent to that of 216 relaxations on the finest grid level. A comparison of Figures 8 and 9 shows that the V(1,n) cycle yields better convergence than the V(n,1) cycle when n is greater than 2. This can be explained in the following manner.

A prolongation from level k to k-1 introduces high frequency errors at level k-1. This is illustrated schematically in Figure 10 for linear interpolation. Level k represents a coarse mesh with 2 elements, AC and CE.

Level k-1 represents a fine mesh with 4 elements, AB, BC, CD, and DE. Using a linear prolongation, the displacements on level k-1 at B and D are found as $w_B = (w_A + w_C)/2$ and $w_D = (w_C + w_E)/2$ with similar expressions for the rotations at B and D. The errors in the displacements at B and D are larger than at C and E, as shown in the Figure 10(b). The total error can be represented as a low frequency (smooth) error plus high frequency (oscillatory) errors. These high frequency errors can be easily eliminated on level k-1 with a few relaxations. The V(1,n) cycle does precisely this, and hence the better convergence compared with the V(n,1) cycle.

Energy-Conserving Prolongation

Figure 11 shows the variation of the L_2-norm as a function of the number of V-cycles for the $V(1,n_1)$ cycle with $n_1 = 1, 2, \ldots, 5$ and $P = R^T$ (energy-conserving prolongation). The larger the value of n_1, the faster the solution converges. For n_1 equal to 3, 4 or 5, the multigrid results converge to the exact solution within the accuracy of the machine in approximately 8 V-cycles with a work equivalent to about 96, 80 or 64 relaxations on the finest grid. For n_1 equal to 1 and 2, slightly more V-cycles were required for convergence for a work expenditure equivalent to 48 and 60 iterations, respectively, on the finest grid. Thus, although for n_1 equal to 1 or 2, more V-cycles are required for convergence, less work is needed than when n_1 is equal to 3, 4 or 5.

The energy-conserving prolongation ($P = R^T$) was also used with the V(n,1) cycle. Two cases are compared in Figure 12. The results for the V(n,1) cycle are virtually identical to those for the V(1,n) cycle. This is expected since the energy-conserving prolongation introduces little or no high frequency errors from the coarse level to the fine level.

Figure 13 compares the exact solution to the multigrid solution for energy-conserving prolongation with the V(2,1) cycle. Figure 13 shows e_w and e_θ, the errors in w and θ, respectively, where e_w and e_θ are calculated as

$$e_w = \frac{w(x) - w(x)_{exact}}{w_{max}} \qquad e_\theta = \frac{\theta(x) - \theta(x)_{exact}}{\theta_{max}}$$

Here w_{max} and θ_{max} are the maximum values of the exact solution. Figure 13 shows e_w and e_θ at the end of the first, third, fifth, and seventh V-cycles. After each V-cycle, the maximum error drops significantly, and after the seventh cycle, the multigrid solution has converged to the exact solution (within machine accuracy).

Red-Black Ordering

To study the performance of the red-black ordering scheme in the $V(n_1,n_2)$ multigrid cycle, all the even-numbered nodes were designated as red and all the odd-numbered nodes were designated black. At each grid level, all the red nodes were relaxed first, followed by the black nodes, in a V(1,1) cycle. For both the linear and energy-conserving prolongations, the solution converged within machine accuracy in a single V-cycle. Thus, with the red-black ordering, convergence is obtained with a work equivalent to only 4 relaxations on the fine grid. The excellent performance of the red-black ordering scheme for this one-dimensional problem is expected and can be explained by a cyclic reduction method.

In the cyclic reduction method, the displacement and rotation at node i (red node) can be expressed in terms of the displacements and rotations at nodes i-1 and i+1 (black nodes), and the node i displacement and rotation can be eliminated from the system. This can be done for all the red nodes, thus

producing a much smaller set of equations. The same procedure can be employed repeatedly until only one or two nodes remain. The solution for the original system is then found by reversing the process. This type of process, which can be applied only to one-dimensional problems, always produces an exact solution in one cycle. For this problem, the current process with red-black ordering is exactly equivalent to this cyclic reduction scheme, and thus converges in one cycle.

CONCLUDING REMARKS

Multigrid procedures were developed for use in one-dimensional finite element analysis. Several aspects of the multigrid procedure were studied and explained in detail.

The key elements of the multigrid method are the restriction and the prolongation operators. These operators were derived based on energy principles. A general procedure for obtaining the restriction matrix was outlined. This procedure considered the residuals from the iterative solution as the loads on the fine grid and transferred these loads, in an energy-conserving manner, onto the coarse grid. The procedure outlined here can be used with any multigrid finite element procedure.

Various aspects of the V-cycle multigrid algorithm were studied in the analysis of the deflections of a one-dimensional, simply supported Bernoulli-Euler beam. From this study, for six grid levels with 32 elements in the finest grid, the following conclusions were drawn.

1. With linear prolongation and sequential ordering, the multigrid algorithm yielded results which were of machine accuracy with work equivalent to about 200 standard Gauss-Seidel relaxations on the finest grid.

2. With linear prolongation and sequential ordering, the V(1,n) cycle with n greater than 2 yielded better convergence rates than the V(n,1) cycle.
3. Maintaining an energy balance during the inter-grid transfers required that the prolongation operator be the transpose of the restriction operator.
4. The multigrid algorithm showed improved convergence rates when energy was conserved in the inter-grid transfers. With the energy-conserving prolongation and sequential ordering, the multigrid algorithm yielded results which were of machine accuracy with a work equivalent to about 50 standard Gauss-Seidel relaxations on the finest grid.
5. The red-black ordering of the relaxation with either the linear or energy-conserving prolongation yielded solutions with machine accuracy in a single V(1,1) cycle. This is equivalent to performing about 4 relaxations on the finest grid level.

REFERENCES

1. Brandt, A.: Multigrid Techniques: 1984 Guide with Applications to Fluid Dynamics. Monograph. Available as GMD-Studie No. 85. from GMD-F1T, Postfach 1240, D-5205, St. Augustin 1, W. Germany.

2. Jameson, A.: Solution of the Euler equations for two dimensional transonic flow by a multigrid method. Applied Math. and Comp., v. 13, pp. 327-355, 1983.

3. Southwell, R. V.: Stress calculation in frameworks by the method of systematic relaxation of constraints. I, II, Proc. Roy. Soc. London Ser. A, 151, pp. 56-95, 1935.

4. Fedorenko, R. P.: The speed of convergence of an iterative process. U.S.S.R. Computational Math. and Math. Phys., v. 4, no. 3, pp. 227-235, 1964.

5. Bakhvalov, N. S.: A relaxation method for solving elliptic equations. U.S.S.R. Computational Math. and Math. Phys., v. 1, no. 5, pp. 1092-96, 1962.

6. Wachpress, C. B.: Iterative Solution of Elliptic Systems. Prentice-Hall Inc., Englewood Cliffs, N. J., 1966.

7. Brandt, A.: Multi-level adaptive solutions to boundary value problems. Math. Comp. 31, ICASE Report 76-27, pp. 333-390, 1977.

8. Nicolaides, R. A.: On the ℓ^2 convergence of an algorithm for solving finite element equations. Math. Comp., 31, pp. 892-906, 1977.

9. Hackbush, W.: On convergence of a multi-grid iteration applied to finite element equations. Report 77-8, Institut für Angewandte Mathematik, Universität Köln, 1977.

10. Stuben, K. and Trottenburg, U.: "Multigrid methods: fundamental algorithms, model problem analysis and applications." Multigrid Methods. W. Hackbush and U. Trottenburg (eds.), Lecture Notes in Math. 960, Springer-Verlag, pp. 1-176, 1982.

11. Hackbush, W.: "Multigrid convergence theory," Multigrid Methods. W. Hackbush and U. Trottenburg (eds.), Lecture Notes in Math. 960, Springer-Verlag, pp. 177-219, 1982.

12. Hackbush, W.: "Parabolic multi-grid methods," Computing Methods in Applied Sciences and Engineering VI, R. Glowinski and J.-L. Lions (eds.), North-Holland, pp. 189-198, 1984.

13. Hackbush, W. and Trottenburg, U. (eds.): Multigrid Methods, Lecture Notes in Math. 960, Springer-Verlag, 1982.

14. Holstein, H. and Paddon, D. (eds.): Multigrid methods for integral and differential equations. Clarendon Press, 1985.

15. McCormick, S. and Trottenburg, U. (eds.): Applied Math. and Comp., Special Issue: Multigrid Methods, v. 13, no. 3 and 4, 1983.

APPENDIX A - BEAM ELEMENT SHAPE FUNCTIONS

For an element with two nodes (four unknowns), the deflected shape w can be assumed to be given by a cubic function, i.e.,

$$w = \alpha_1 + \alpha_2 x + \alpha_3 x^2 + \alpha_4 x^3 \qquad 0 \leq x \leq b \qquad \text{(A1)}$$

Equation (A1) can be written in terms of shape functions N_i (i = 1 to 4) corresponding to w_j and θ_j (j = 1,2) as follows:

$$w(x) = w_1 N_1 + \theta_1 N_2 + w_2 N_3 + \theta_2 N_4 \qquad \text{(A2)}$$

where

$$N_1 = 1 - \frac{3x^2}{b^2} + \frac{2x^3}{b^3} \qquad N_2 = x - \frac{2x^2}{b} + \frac{x^3}{b^2}$$

$$0 \leq x \leq b \qquad \text{(A3)}$$

$$N_3 = \frac{3x^2}{b^2} - \frac{2x^3}{b^3} \qquad N_4 = -\frac{x^2}{b} + \frac{x^3}{b^2}$$

Here b is the element length.

The element stiffness matrix, obtained from these shape functions, is given in the text (equation (4)).

APPENDIX B - CONVERGENCE OF THE GAUSS-SEIDEL METHOD

The Gauss-Seidel iterations efficiently remove the high frequency errors but not the low frequency errors. This appendix demonstrates the efficiency of Gauss-Seidel iterations in removing the high frequency errors and discusses the convergence of the Gauss-Seidel method.

Figures B1 and B2 show the efficiency of the Gauss-Seidel method in removing the high frequency errors. A random initial approximation was used for these figures. The displacement w at each node, normalized by the exact displacement at the center of the beam, is shown at the end of the 1^{st}, 10^{th}, 50^{th}, 1000^{th}, 10000^{th}, and 20000^{th} iteration in Figure B1. Similar information for the rotation θ at each node is given in Figure B2. For both the displacement w and the rotation θ, the majority of the high frequency errors have been smoothed out by the 10^{th} iteration. The remaining smooth errors are not handled efficiently by the Gauss-Seidel method.

Figures B3 and B4 present the iterative solutions for the displacements and rotations for a zero initial approximation. The displacement w at each node, normalized by the exact displacement at the center of the beam, is shown at the end of the 500^{th}, 1000^{th}, 5000^{th}, 10000^{th}, 20000^{th}, and 30000^{th} iteration in Figure B3. Similar information for the rotation θ at each node is given in Figure B4. Here again the Gauss-Seidel method performs very inefficiently.

In fact, the performance of the Gauss-Seidel method is so poor for this example that even after 30000 iterations, the iterative solutions are still grossly in error. Figures B5 and B6 compare the exact solution to the iterative solution for two different initial approximations. Figure B5 shows w, the displacements, and Figure B6 shows θ, the rotations after 30000

iterations. In both figures, the solid line represents the exact solution while the dashed and dash-dot line represent the zero and random initial approximations, respectively. Even after 30000 iterations, the magnitudes of both iterative solutions are grossly in error and, obviously, the nature of the initial approximation still has a large effect on the iterative solution.

The very slow convergence in this problem is also due, in part, to the nature of the stiffness matrix for the beam example. The Gauss-Seidel iterative method works best for diagonally dominant matrices. However, as seen in equation (3), the beam stiffness matrix contains off-diagonals terms of the same or higher order than the diagonals terms. Hence, the poor performance of the Gauss-Seidel in this example is not unexpected.

APPENDIX C - ERROR ANALYSIS

This appendix examines the relationship between the error in the displacements and the error in the L_2-norm of the residuals. As stated previously, although the displacements appeared to have converged to the direct solution within machine accuracy (10^{-14}), the L_2-norm of the residuals was on the order of 10^{-9}. Figure C1 shows the errors in w and θb, normalized by the maximum displacement, where the error in the displacement is computed as the difference between the iterative solution displacement and the direct solution displacement. Figure C2 presents the normalized force and moment residuals along the length of the beam. As seen in Figure C1, the displacement errors are smooth and on the order of 10^{-9}, and while the residuals (Figure C2) are also on the order of 10^{-9}, they are oscillatory.

Consider the equation for the i^{th} residual:

$$r_i = f_i - \sum_{j=1}^{N} k_{ij} v_j \tag{C1}$$

where v_j is the current approximate solution. The term v_j can be expressed as follows:

$$v_j = d_j - e_j \tag{C2}$$

where d_j is the direct displacement solution at node j and e_j represents the error at node j.

Since by definition $f_i = \sum_{j=1}^{N} k_{ij} d_j$, equation (C1) can be rewritten as follows:

$$r_i = \sum_{j=1}^{N} k_{ij} e_j \tag{C3}$$

or,

$$r_i = \sum_{j=1}^{N} k_{ij} e_j \leq \sum_{j=1}^{N} |k_{ij}||e_j| \tag{C4}$$

If all the errors e_j ($j = 1, 2, \ldots, N$) are on the order of e_m, the accuracy of the machine, then the following is true:

$$r_i \leq e_m \sum_{j=1}^{N} |k_{ij}| \tag{C5}$$

To keep the dimensions the same, in the current problem of a one-dimensional beam, the error in w is denoted by e_w while the error in θ is denoted by be_θ. Equation (C5) then reduces to the following:

$$\begin{aligned} r_{w_i} &\leq e_m \frac{EI}{b^3} [12 + 6 + 24 + 12 + 6] \\ r_{\theta_i}/b &\leq e_m \frac{EI}{b^3} [6 + 2 + 8 + 6 + 2] \end{aligned} \tag{C6}$$

So that the residuals of the forces and moments will have the same dimensions, the moment residuals have been divided by b, the element length.

Equations (C6) can be written in a nondimensional form as follows:

$$\begin{aligned} r_{w_i}/(q_0 L) &\leq \bar{e}\, 8(L/b)^3 \\ r_{\theta_i}/(q_0 bL) &\leq \bar{e}\, 24(L/b)^3 \end{aligned} \tag{C7}$$

where $\bar{e} = e_m/d_{max}$ and d_{max} is the maximum displacement from the direct solution of the stiffness equations.

Thus if e_m is on the order of the machine accuracy ($e_m = 10^{-14}$), then the nondimensional residuals for the w and θ degrees of freedom for a beam with 32 elements can be at most 1.96×10^{-8} and 0.786×10^{-8}, respectively. When the residuals are smaller than these maximums, as in Figure C2, the solution displacements have converged within machine accuracy, and no further improvements can be expected.

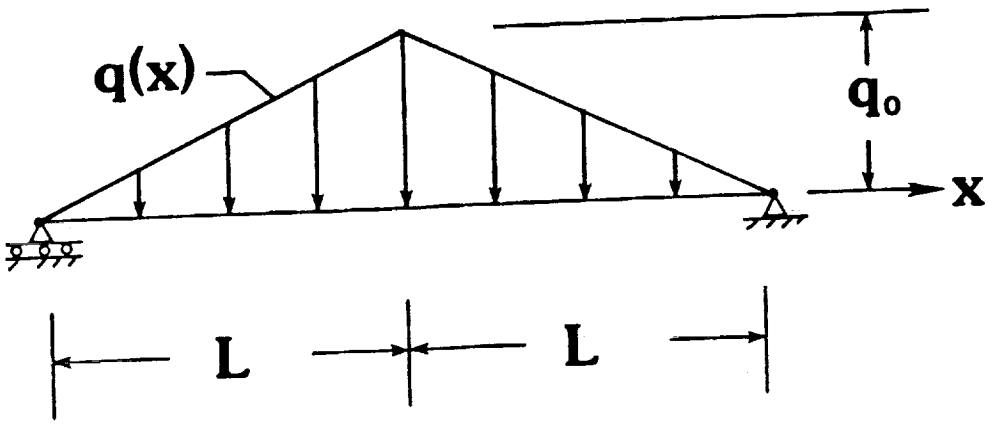

simply supported beam

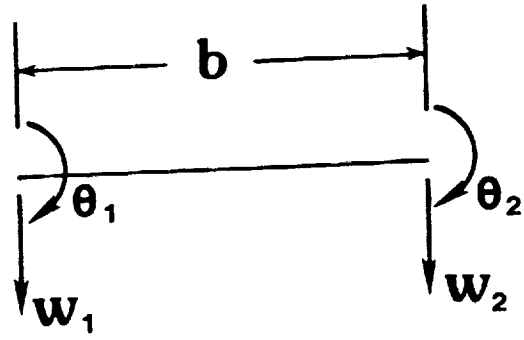

beam element

$$q(x) = \begin{cases} q_0 x/L & 0 \le x \le L \\ q_0(2-x/L) & L \le x \le 2L \end{cases}$$

distributed loading

Figure 1. Simply supported beam under distributed loading.

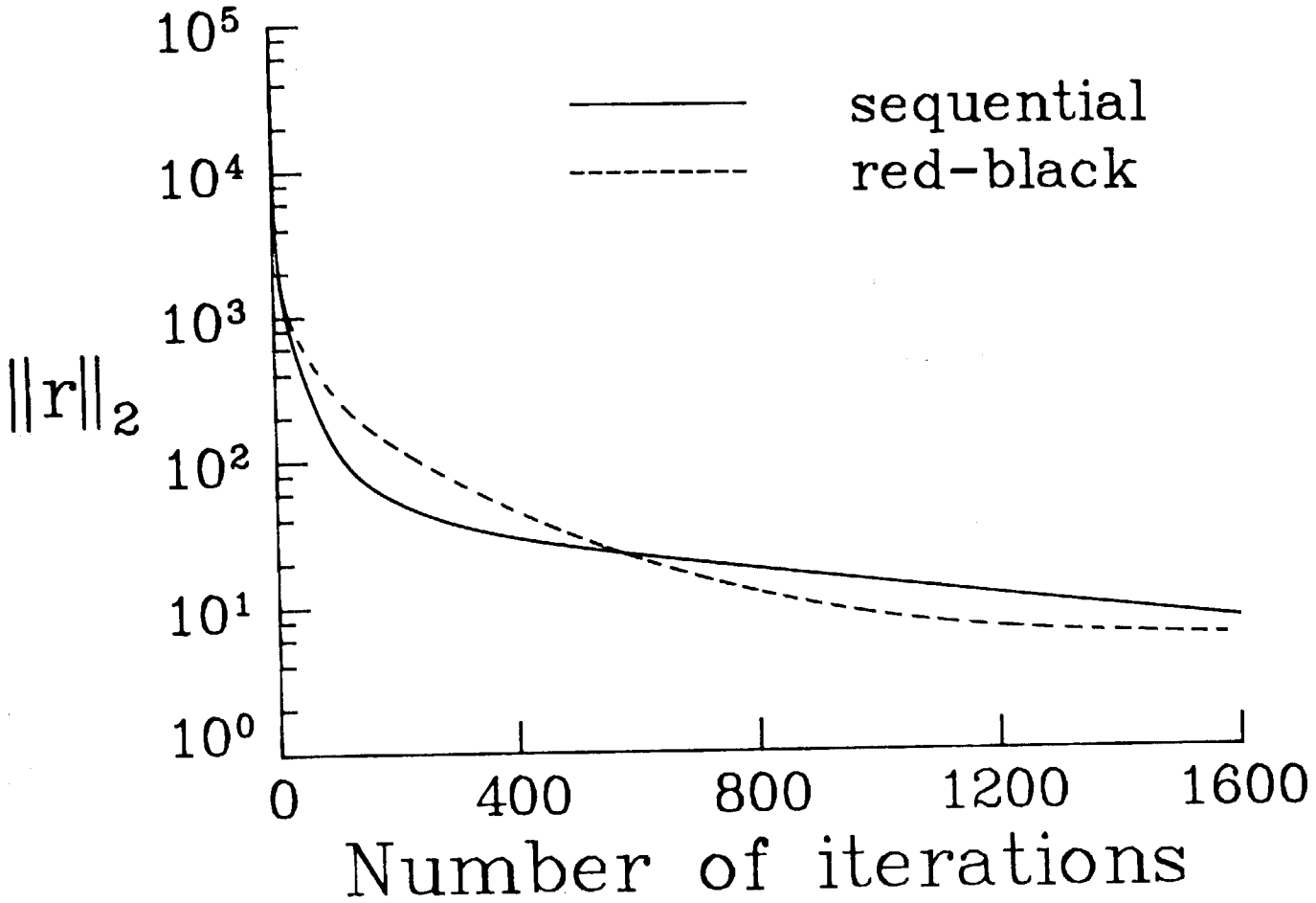

Figure 2. L_2-norm for sequential and red-black ordering of Gauss-Seidel iterations.

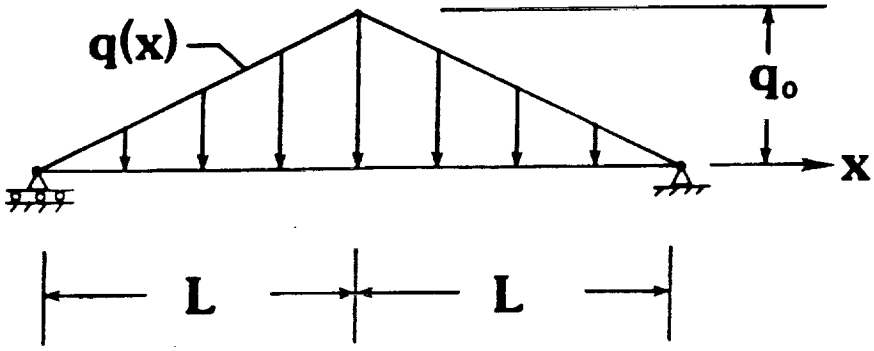

simply supported beam

Grid level	Element size
1	L/32
2	L/16
3	L/8
4	L/4
5	L/2
6	L

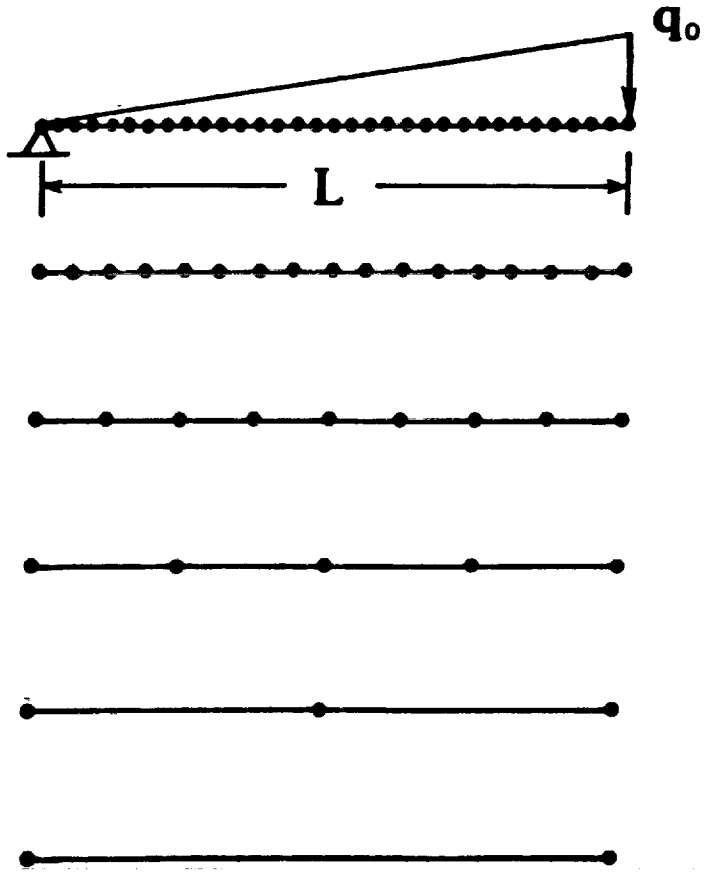

Figure 3. Sequence of grids for simply supported beam.

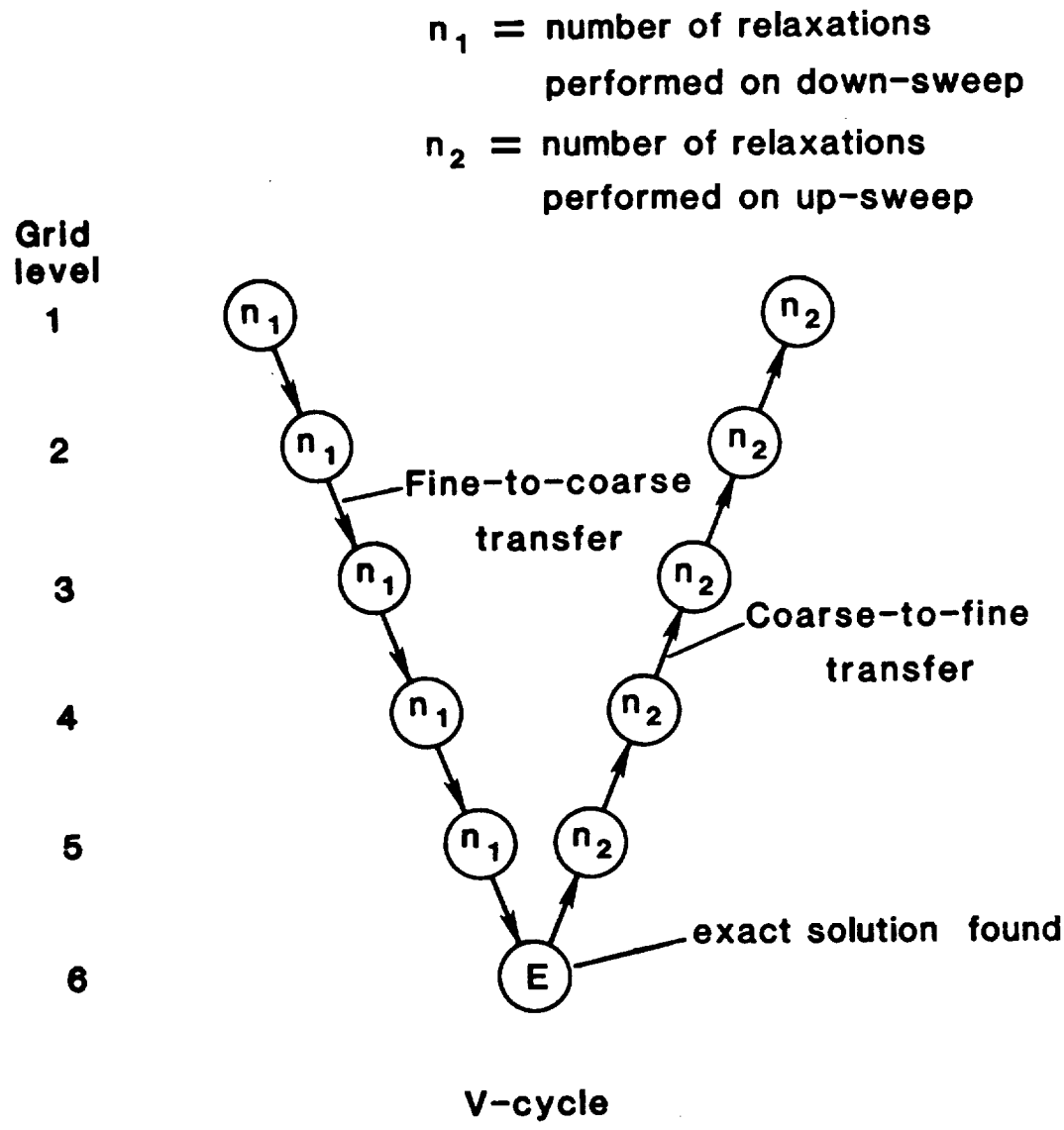

Figure 4. V-cycles for six levels, $V(n_1,n_2)$.

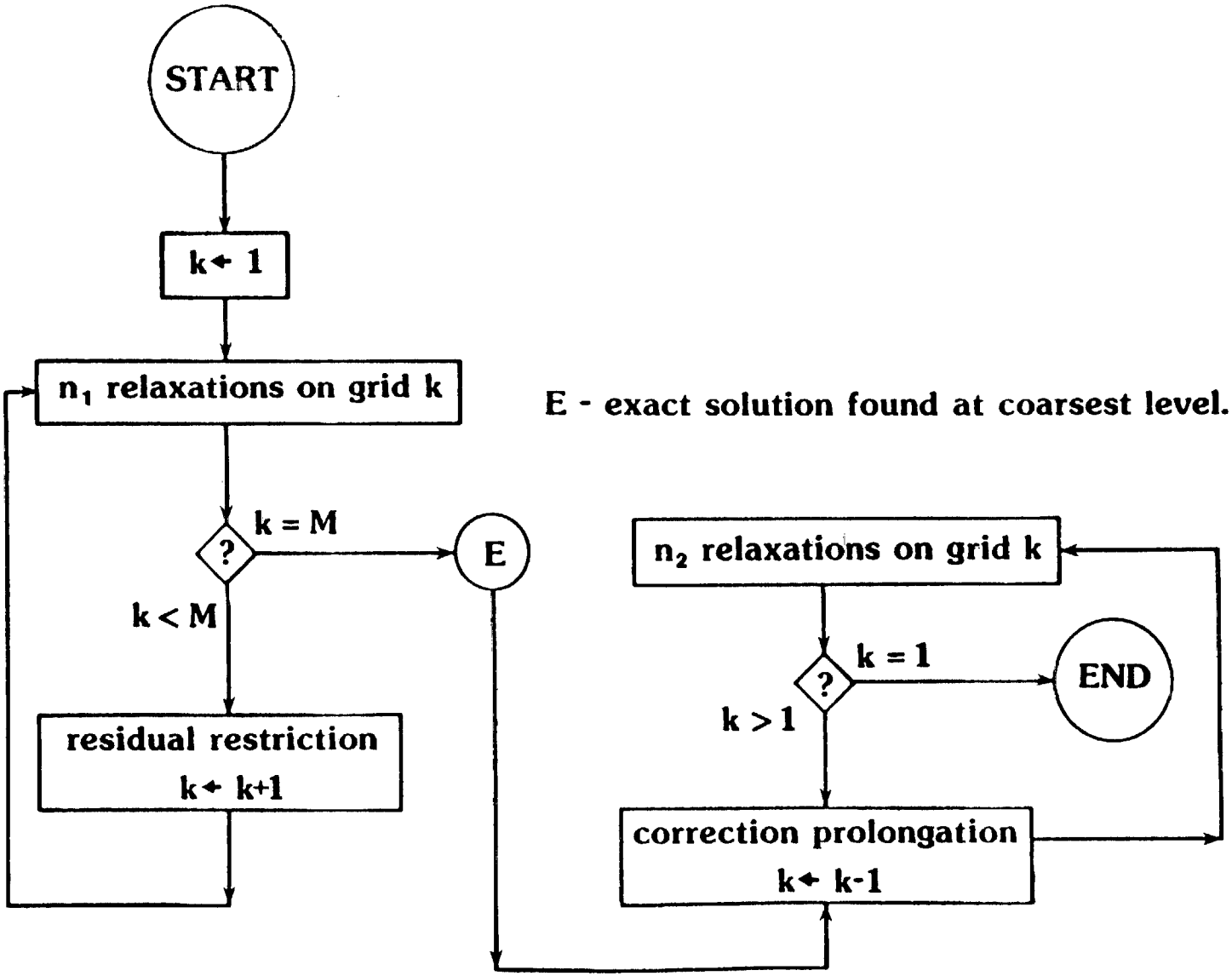

Figure 5. Flowchart of multigrid cycle.

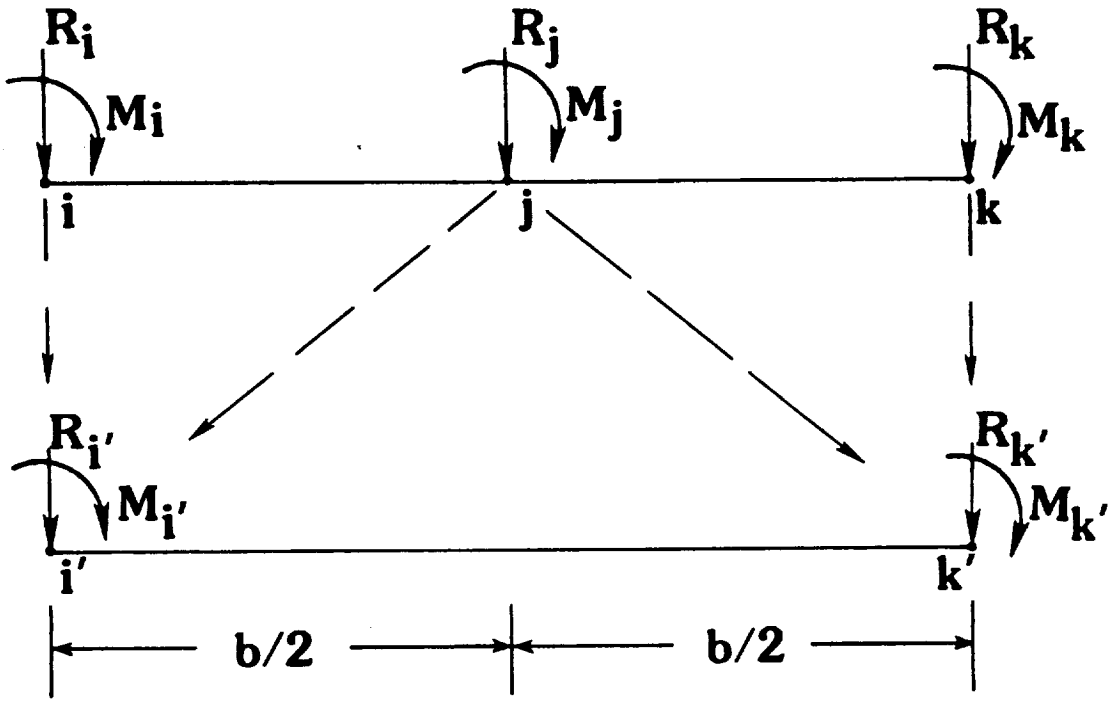

$$R_{i'} = R_i + R_j/2 - 3M_j/(4b) \qquad R_{k'} = R_k + R_j/2 + M_j/(4b)$$

$$M_{i'} = M_i + R_j b/4 - M_j/4 \qquad M_{k'} = M_k - R_j b/4 - M_j/4$$

Figure 6. Consistent transfer of force and moment residuals.

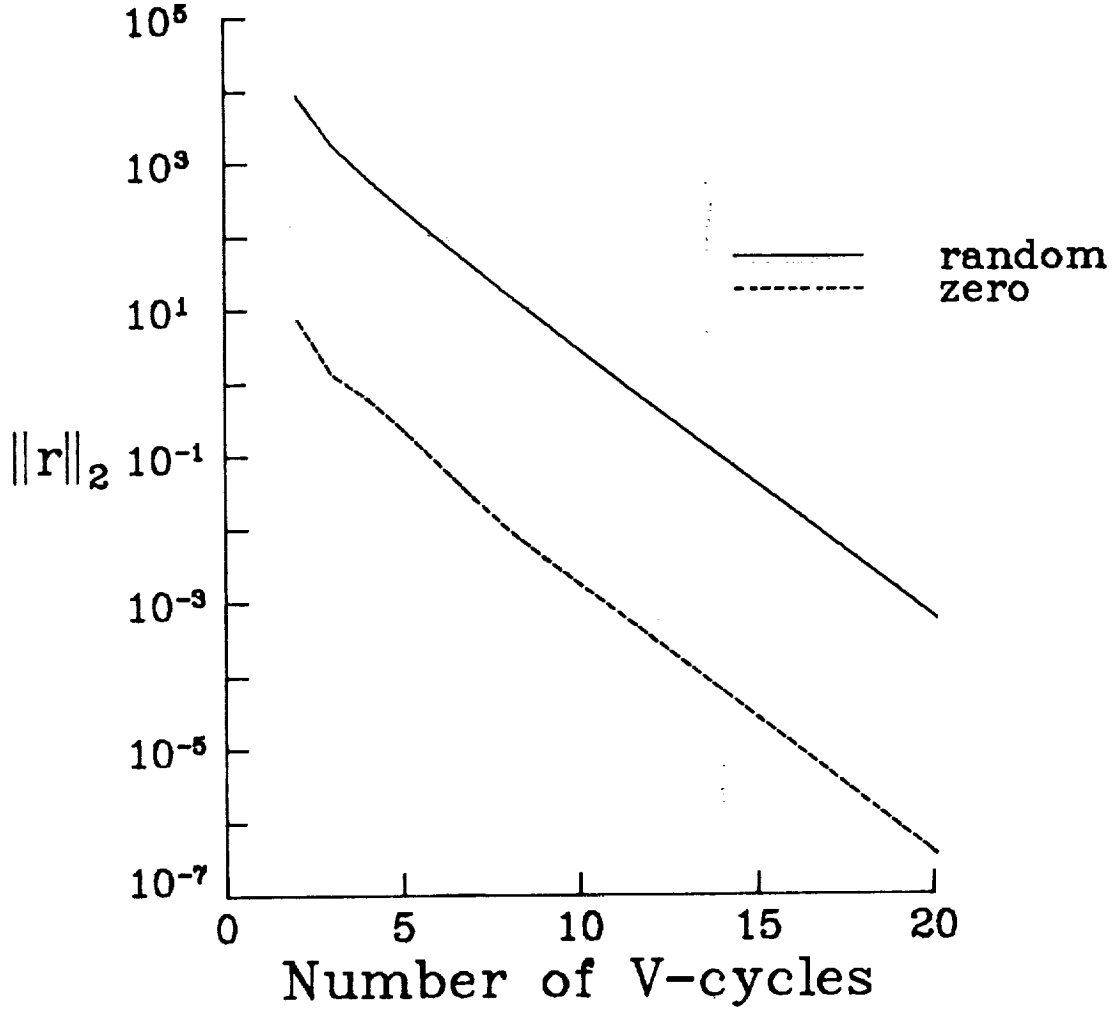

Figure 7. L_2-norm for zero and random initial approximations with linear prolongation and V(1,2) cycles.

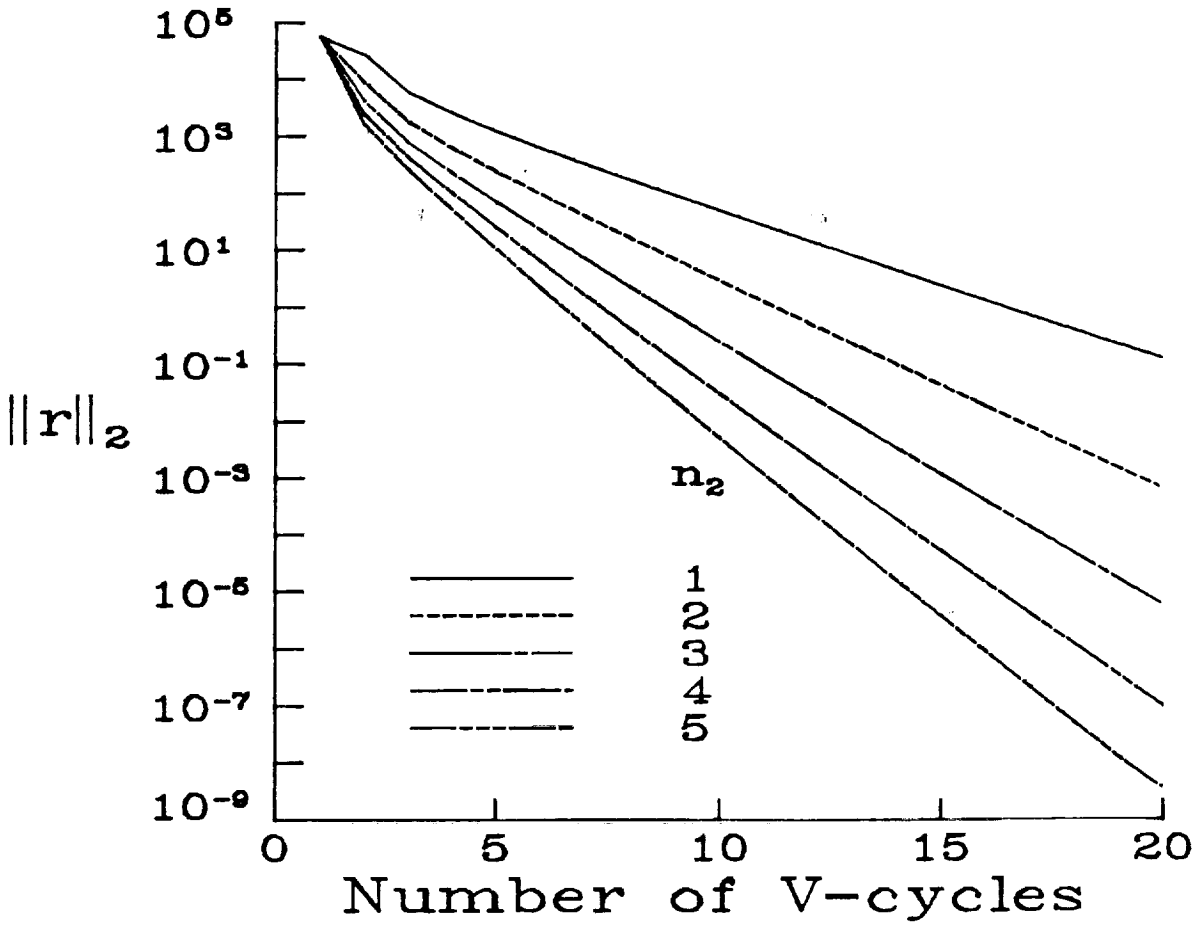

Figure 8. L_2-norm for linear prolongation and $V(1,n_2)$ cycles.

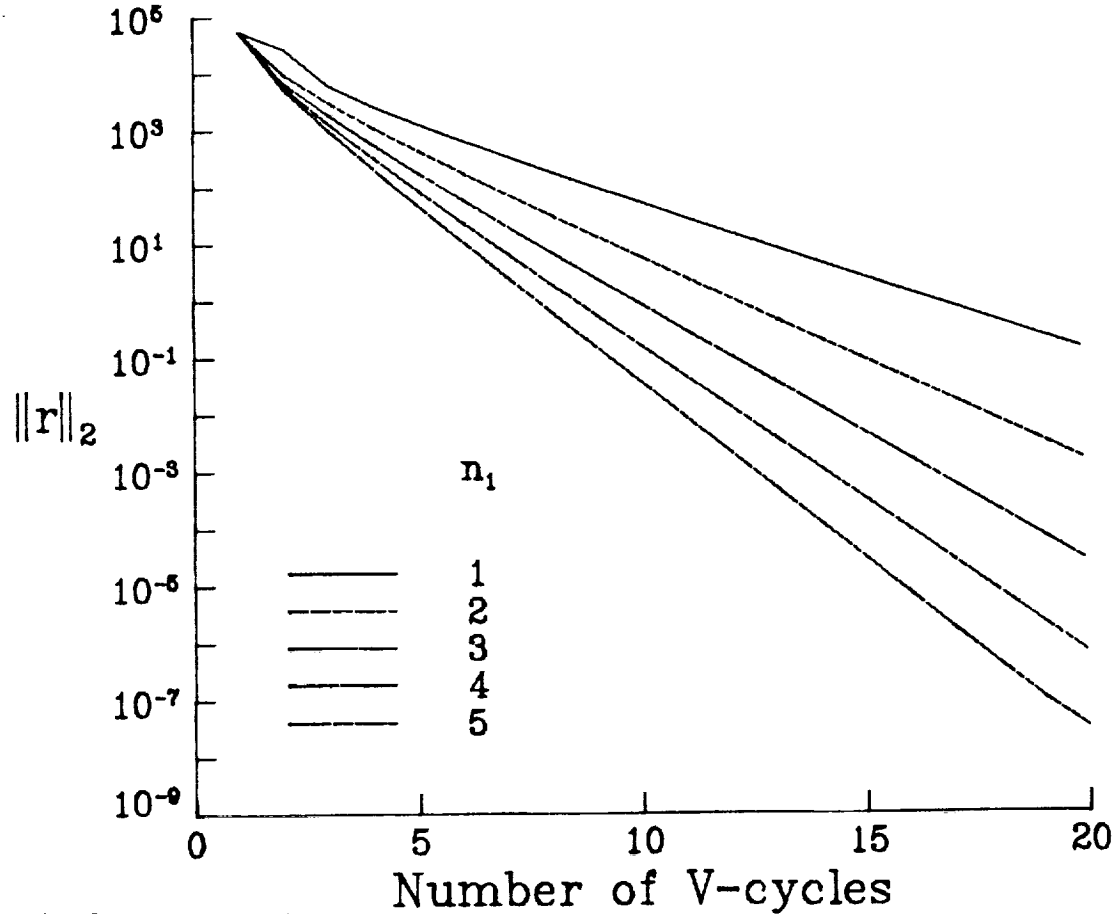

Figure 9. L_2-norm for linear prolongation and $V(n_1,1)$ cycles.

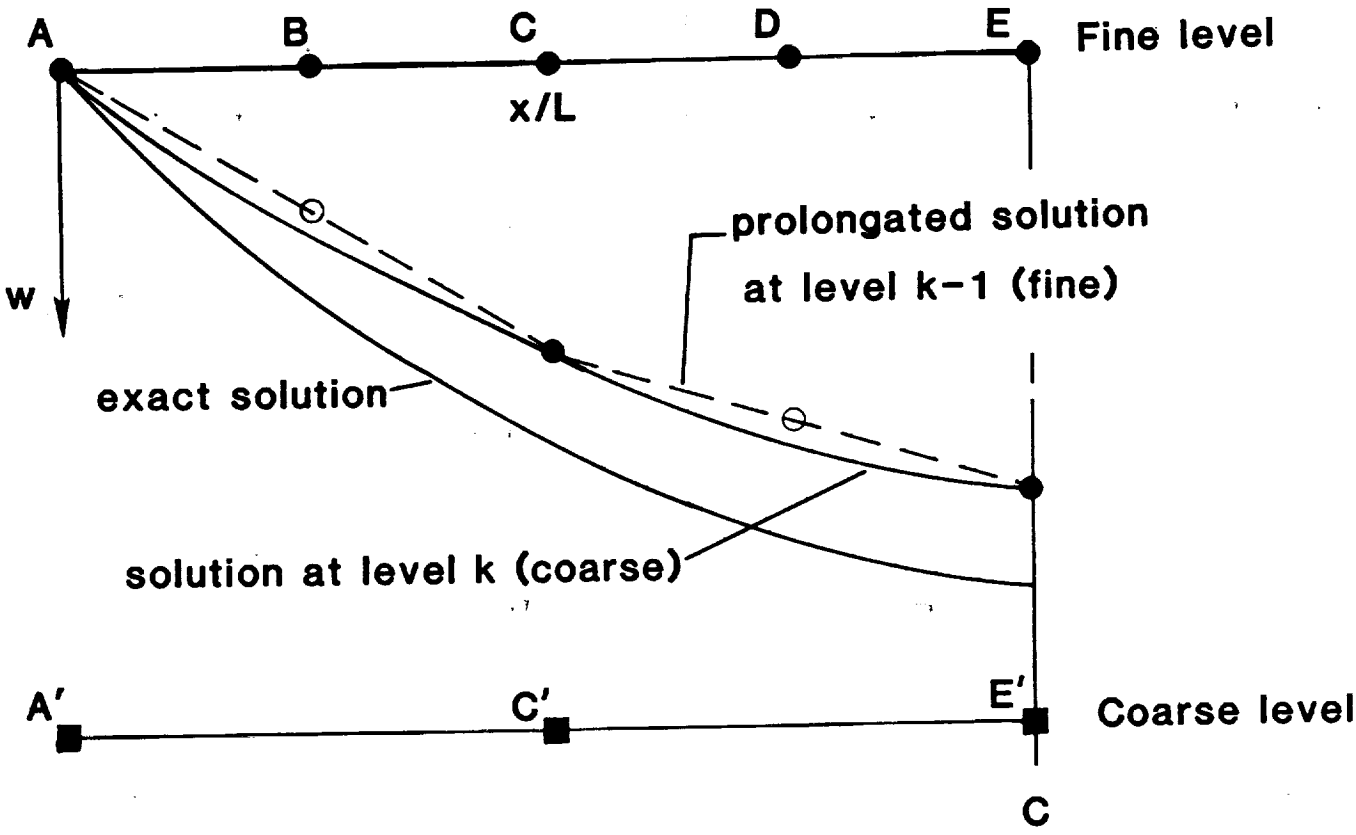

Solutions at level k and k-1.

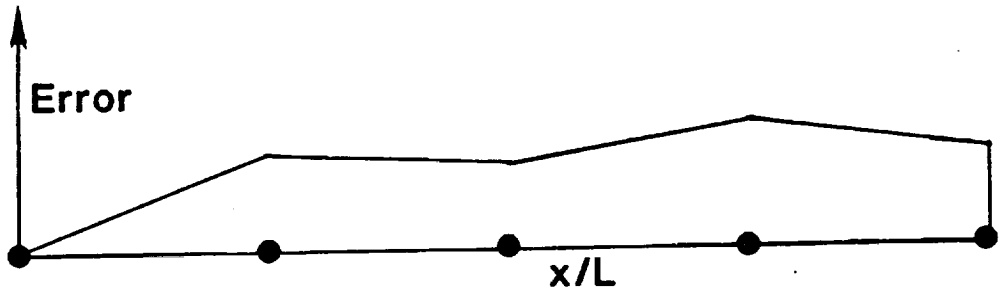

Error in prolongated solution at level k-1 (fine).

Figure 10. High frequency errors due to linear prolongation.

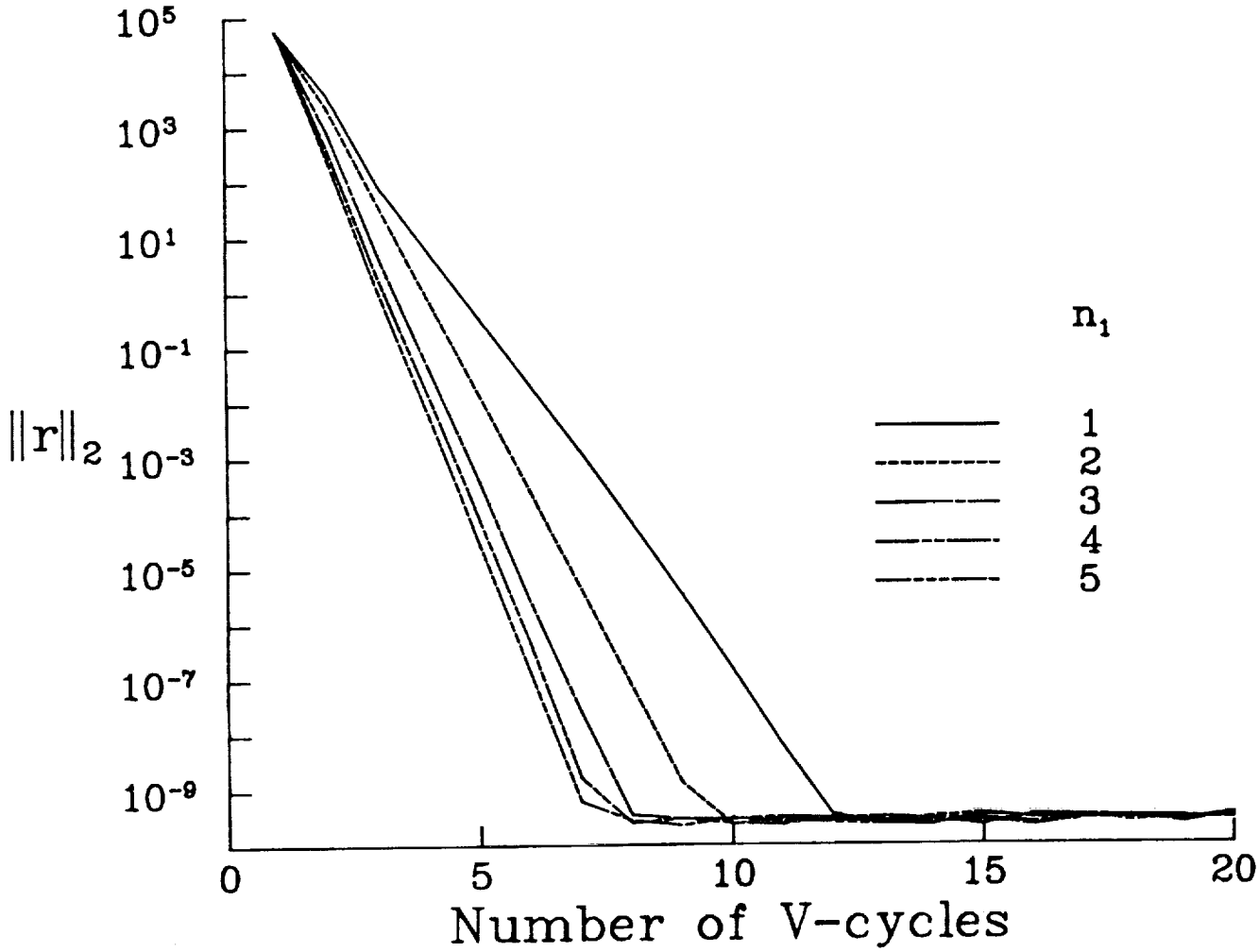

Figure 11. L_2-norm for energy-conserving prolongation and $V(n_1,1)$ cycles.

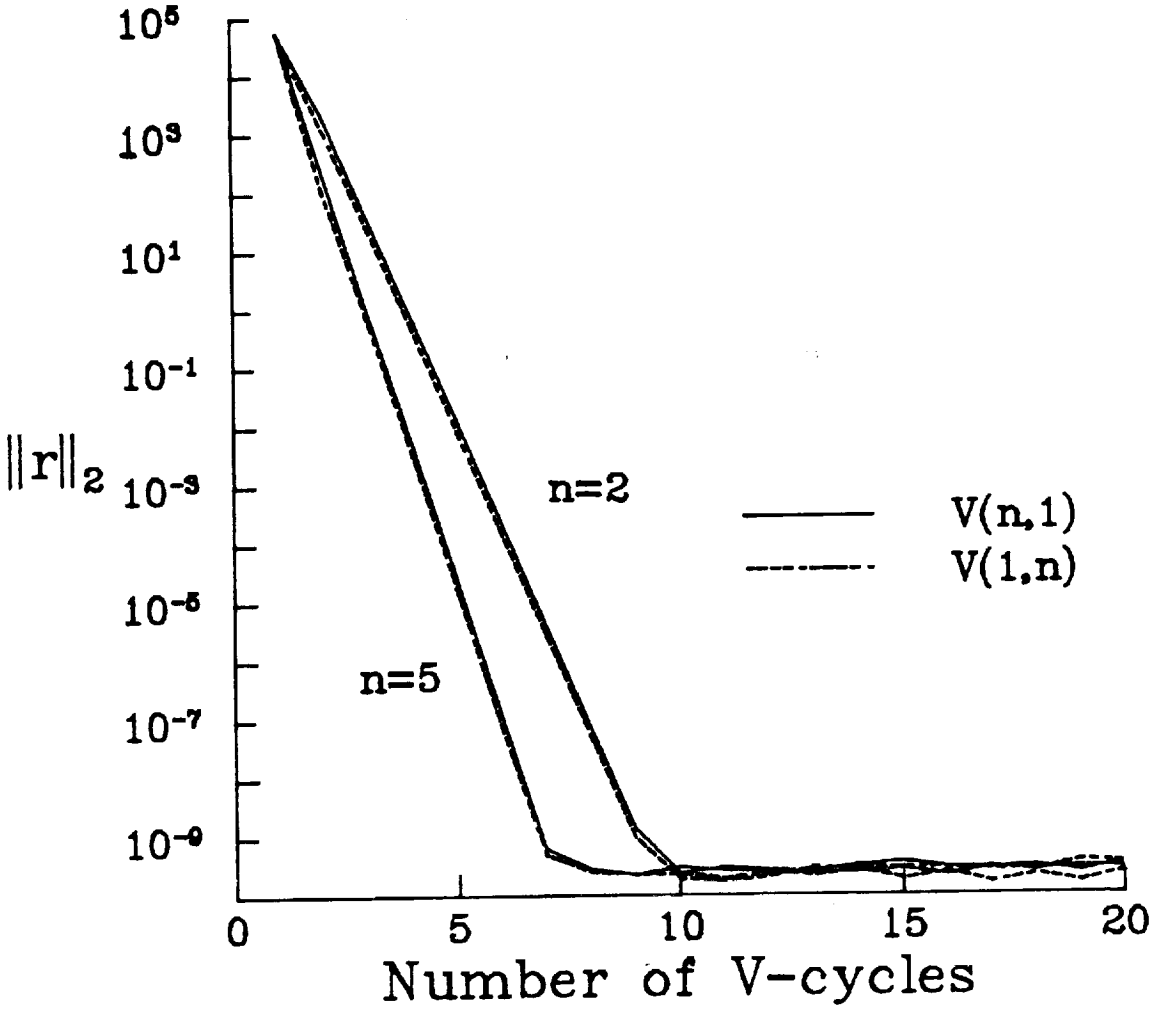

Figure 12. L_2-norm for energy-conserving prolongation.

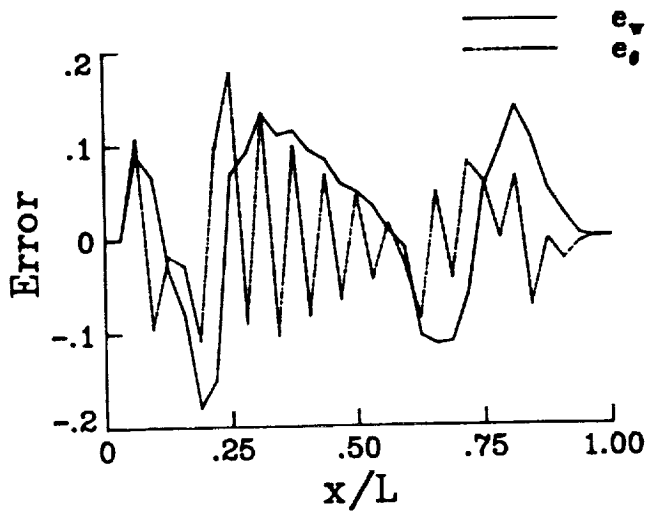

(a) Error after one V-cycle.

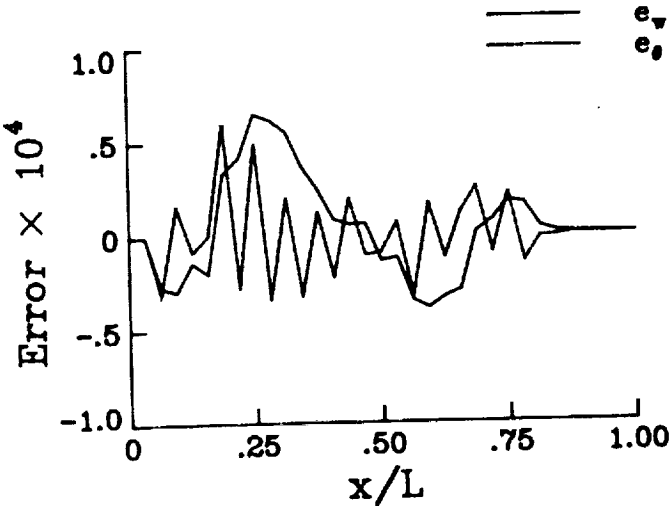

(b) Error after three V-cycles.

Figure 13. Error in multigrid solution for energy-conserving prolongation and V(2,1) cycles.

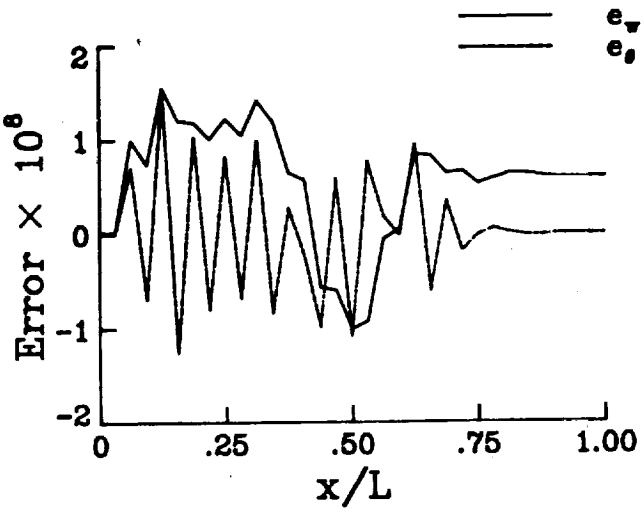

(c) Error after five V-cycles.

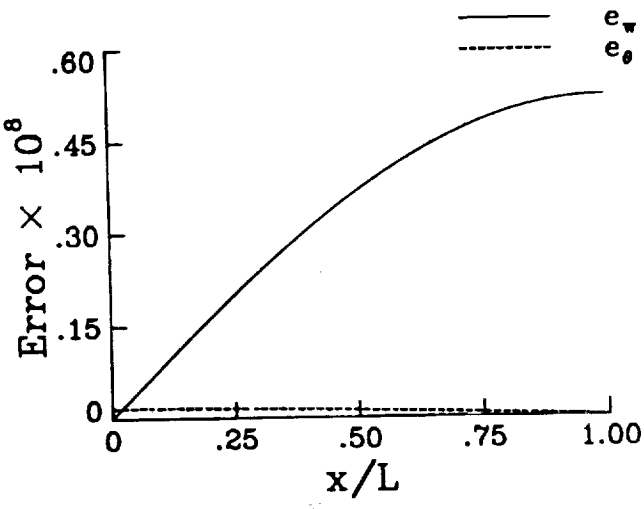

(d) Error after seven V-cycles.

Figure 13. Continued.

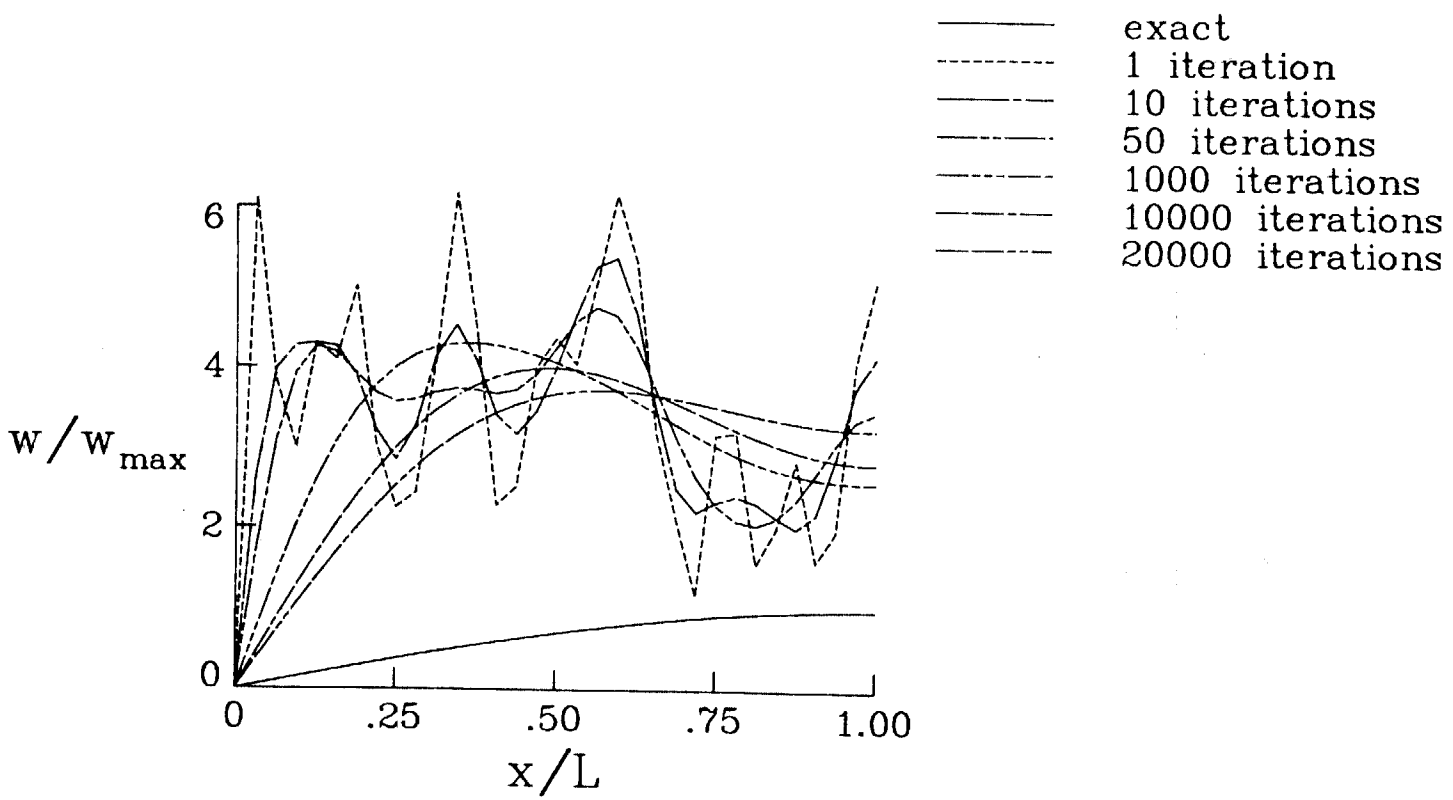

Figure B1. Exact and iterative solutions for deflections with random initial approximation.

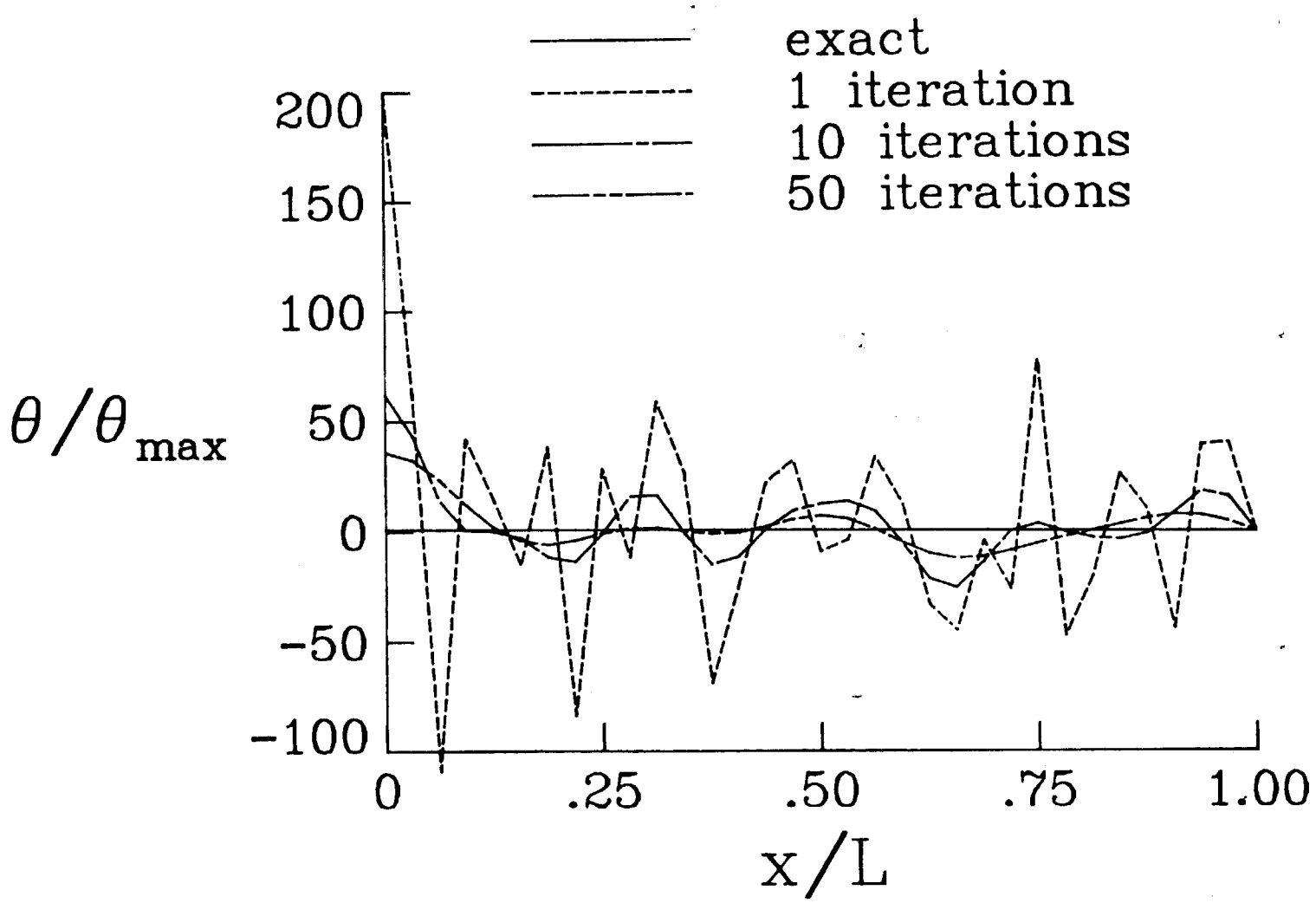

Figure B2. Exact and iterative solutions for rotations with random initial approximation.

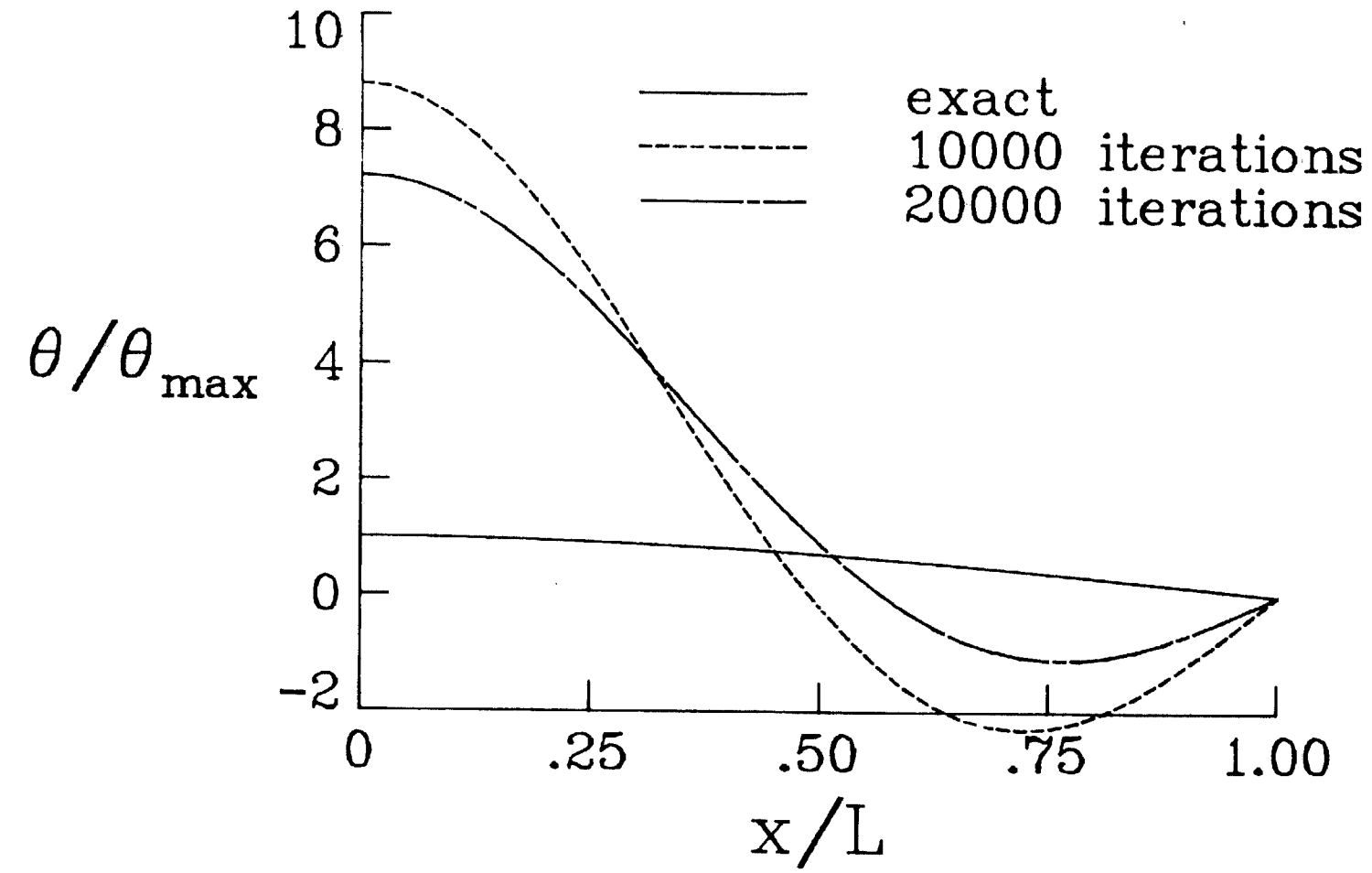

Figure B2. Continued.

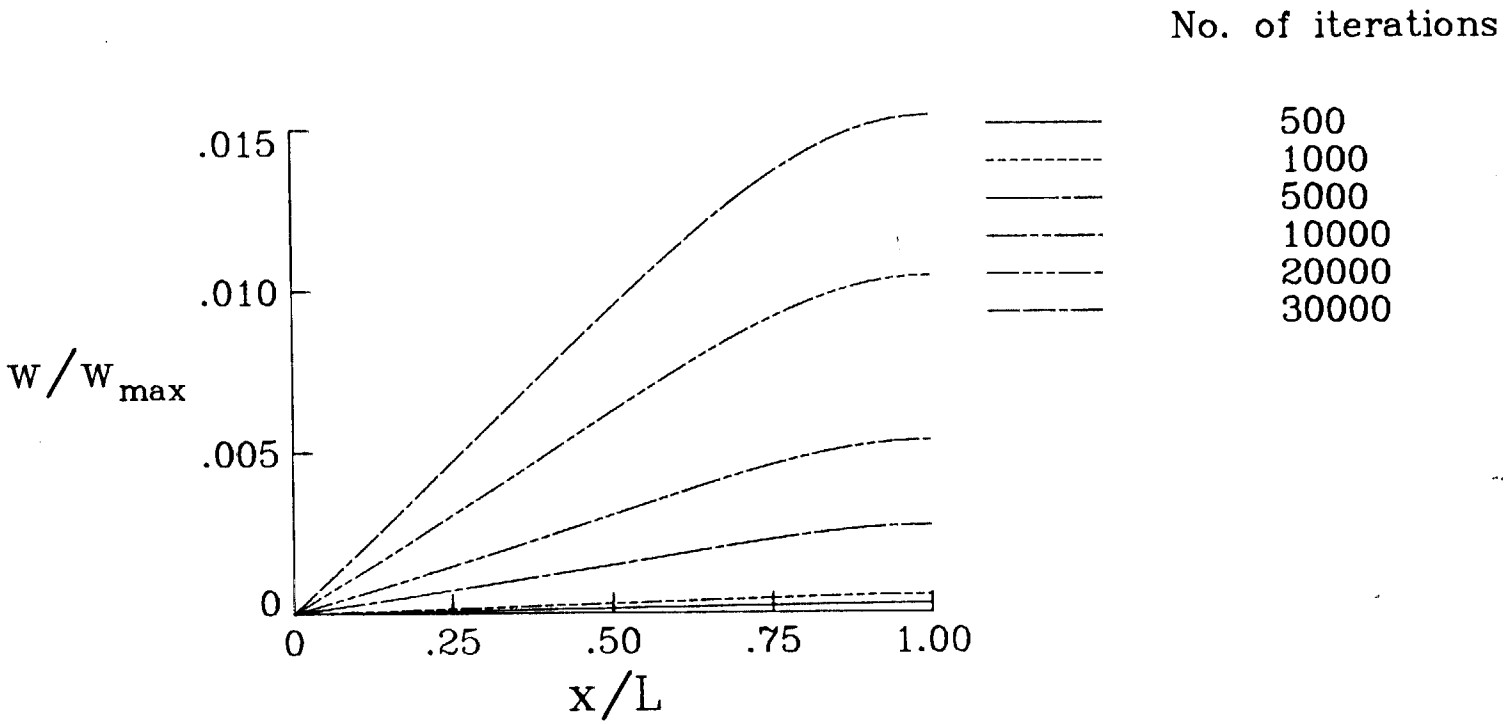

Figure B3. Iterative solution for deflections with zero initial approximation.

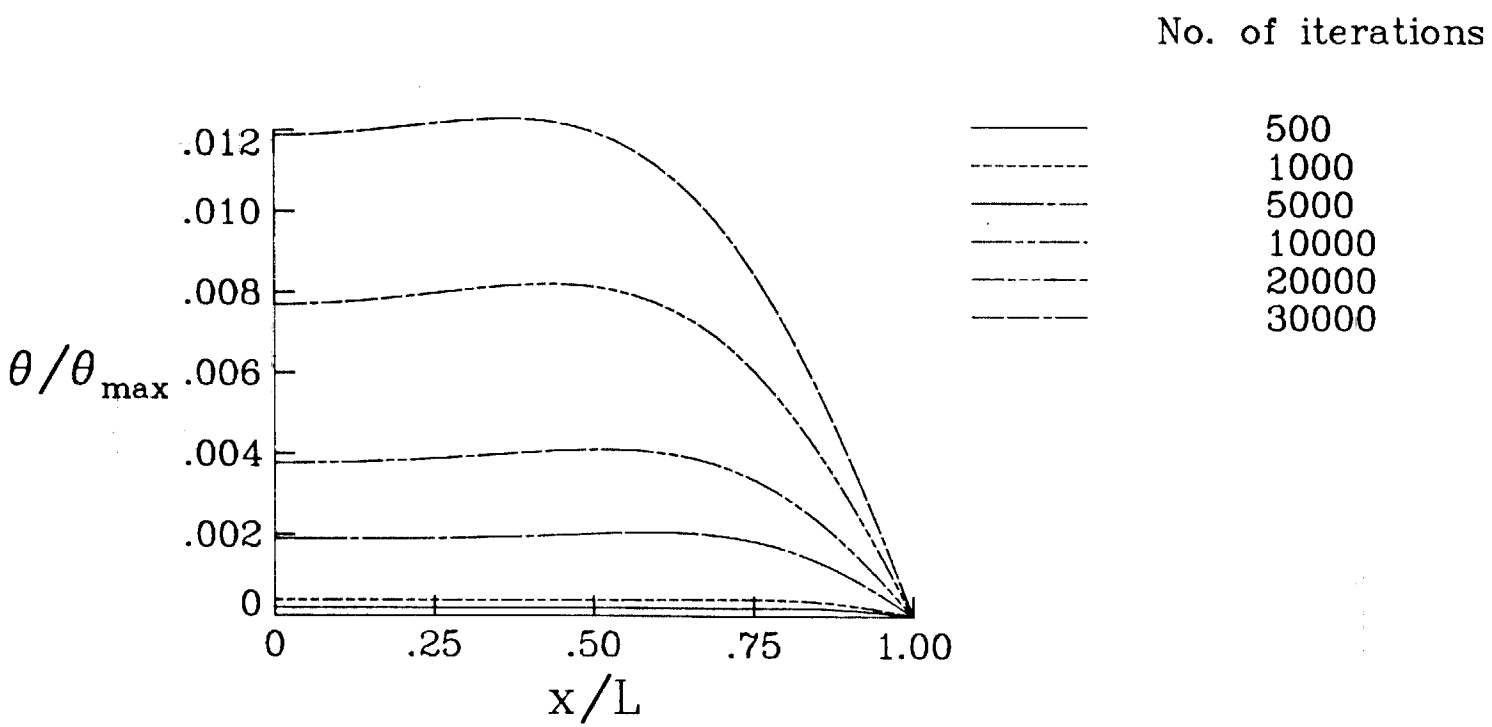

Figure B4. Iterative solutions for rotations with zero initial approximation.

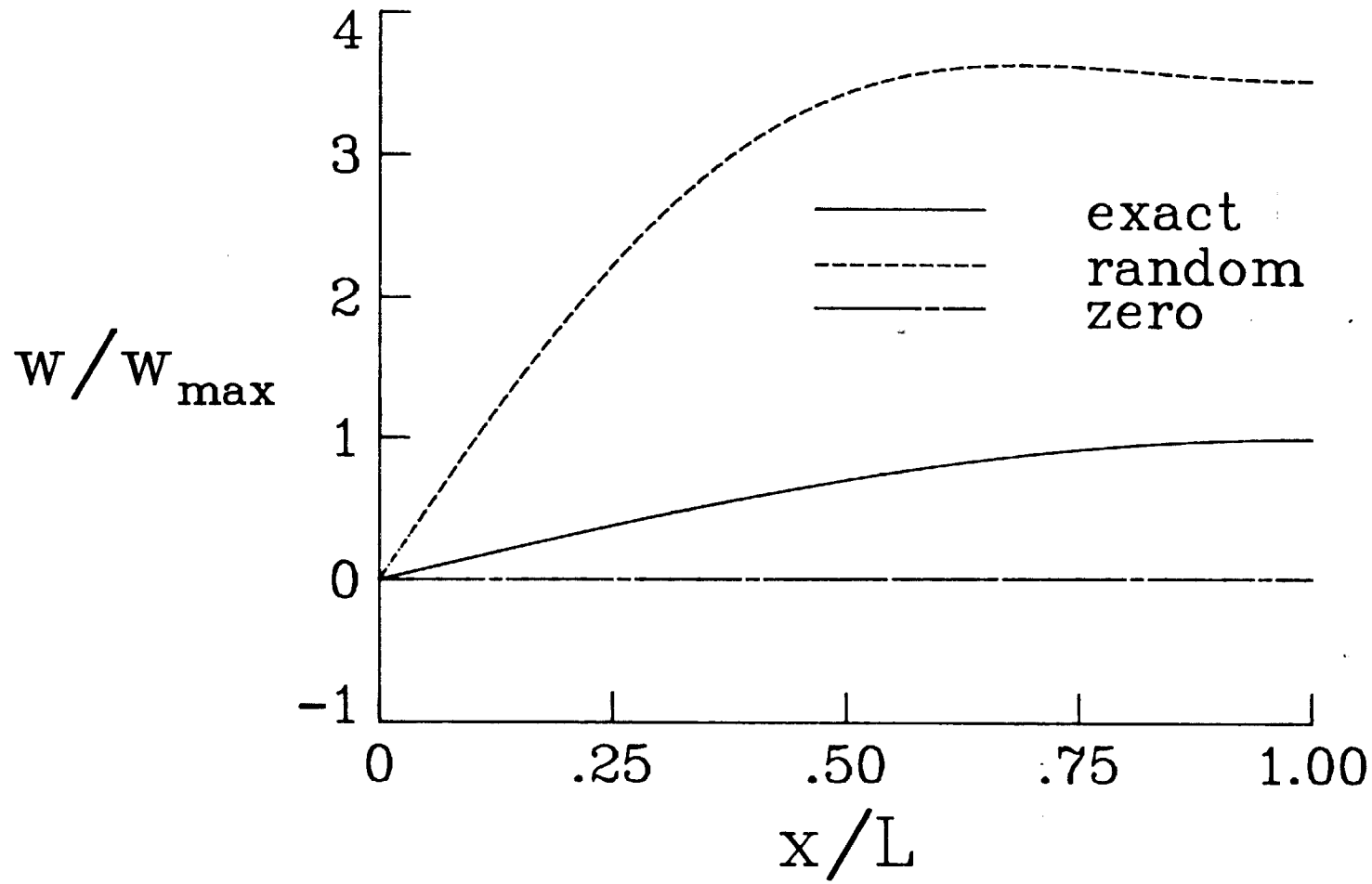

Figure B5. Exact and iterative solutions for deflections after 30000 iterations.

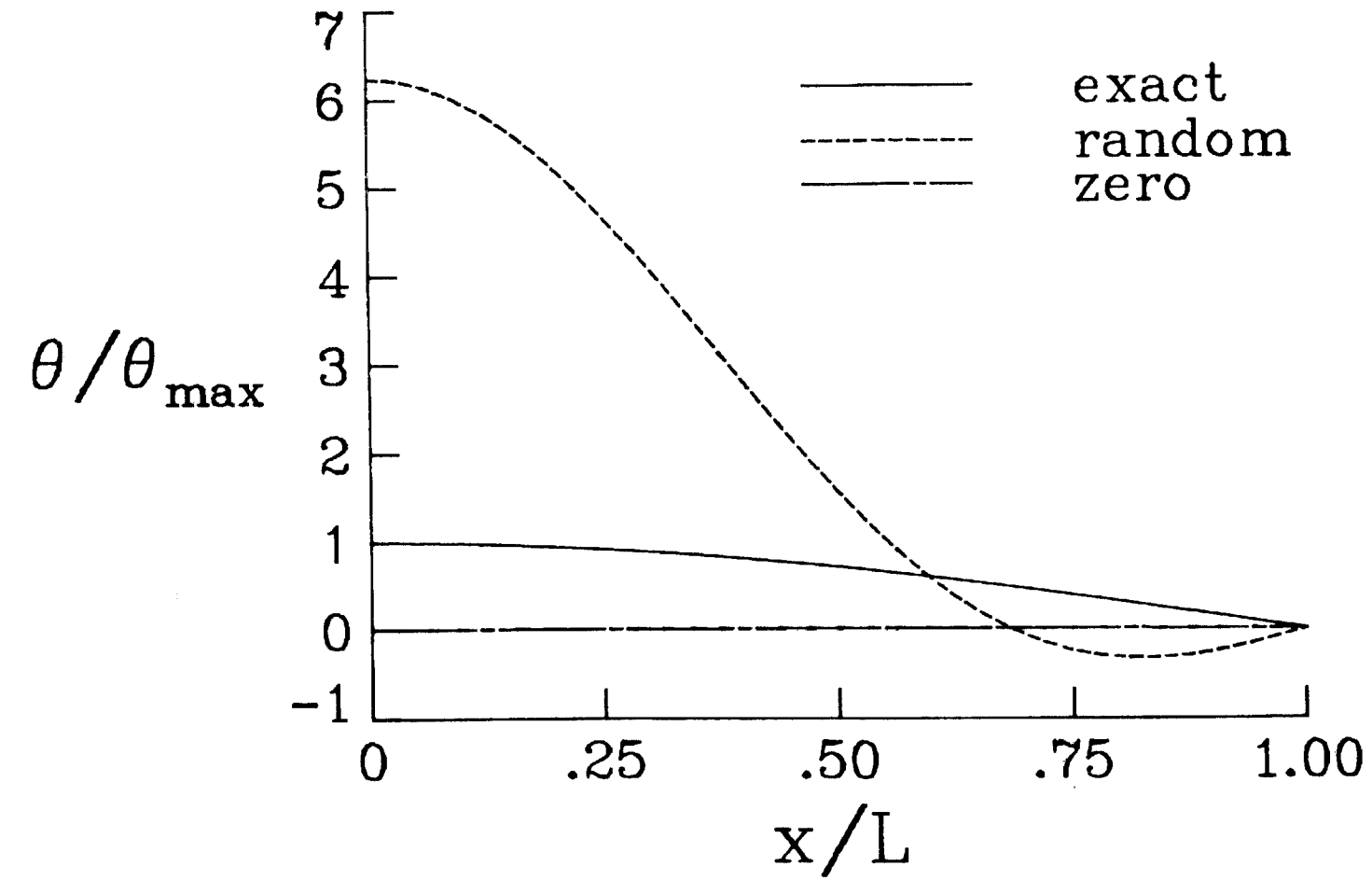

Figure B6. Exact and iterative solutions for rotations after 30000 iterations.

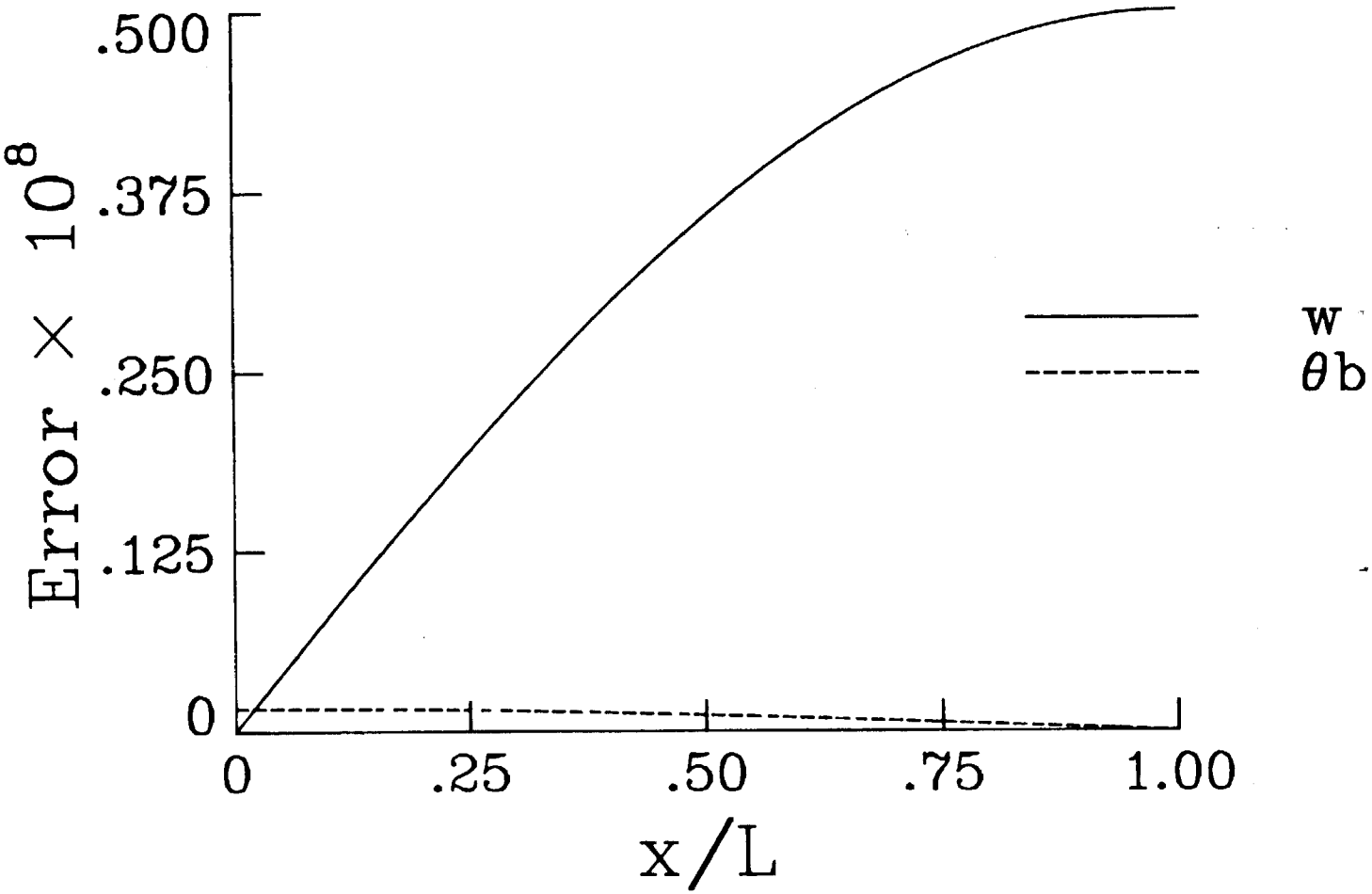

Figure C1. Errors in deflections and rotations.

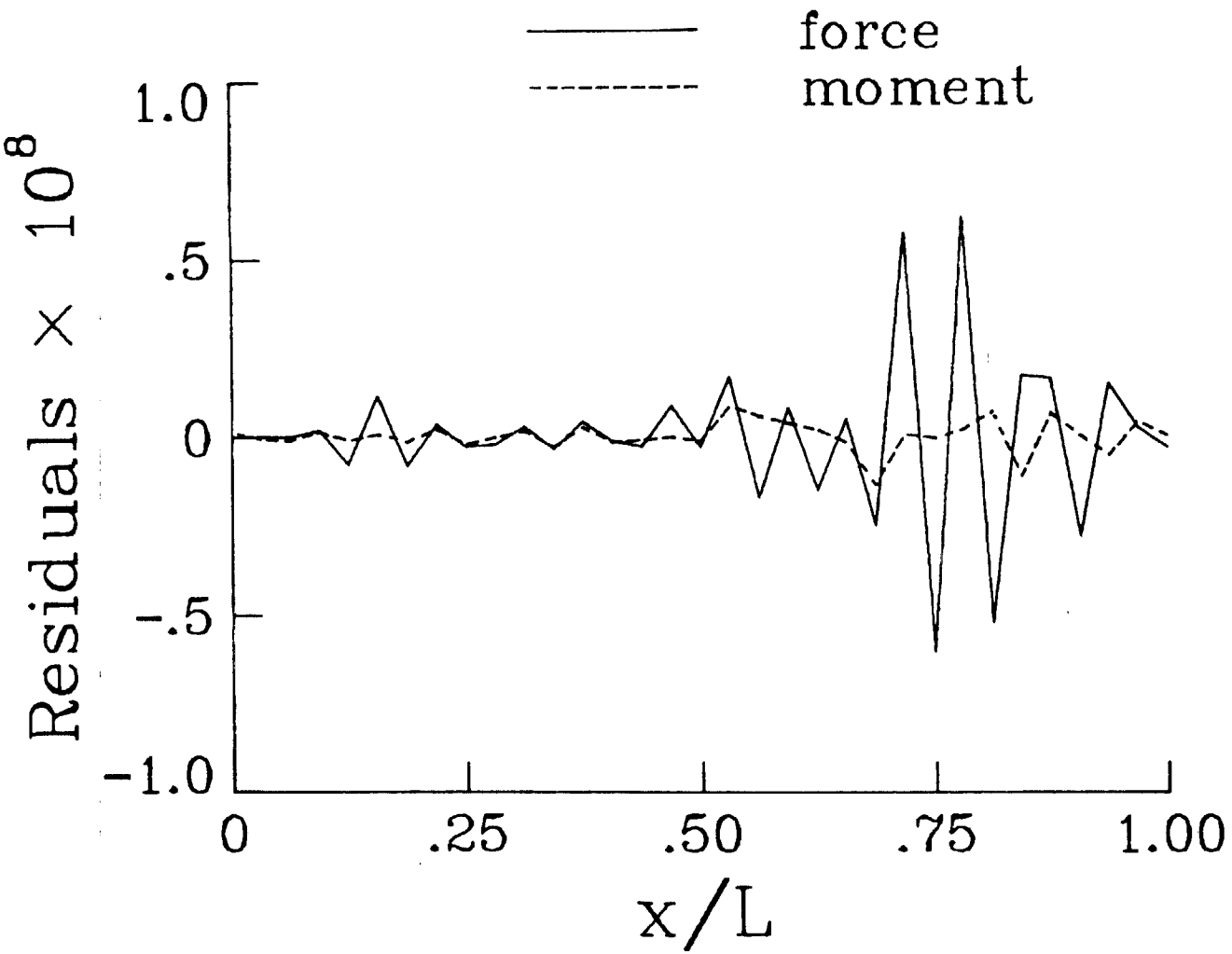

Figure C2. Variations in force and moment residuals.

Standard Bibliographic Page

1. Report No.	2. Government Accession No.	3. Recipient's Catalog No.
NASA TM-87761		

4. Title and Subtitle	5. Report Date
Multigrid Methods in Structural Mechanics	July 1986
	6. Performing Organization Code: 505-63-01

7. Author(s)	8. Performing Organization Report No.
I. S. Raju*, C. A. Bigelow, S. Ta'asan**, M. Y. Hussaini**	

9. Performing Organization Name and Address	10. Work Unit No.
NASA Langley Research Center Hampton, VA 23665-5225	11. Contract or Grant No.

12. Sponsoring Agency Name and Address	13. Type of Report and Period Covered
National Aeronautics and Space Administration Washington, DC 20546-0001	Technical Memorandum
	14. Sponsoring Agency Code

15. Supplementary Notes

A-VC-25068

*Analytical Services & Materials, Inc.; work performed under NAS1-17808

**ICASE, NASA Langley Research Center, work performed under NAS1-17070

16. Abstract

Although the application of multigrid methods to the equations of elasticity has been suggested, few such applications have been reported in the literature. In the present work, multigrid techniques are applied to the finite element analysis of a simply supported Bernoulli-Euler beam, and various aspects of the multigrid algorithm are studied and explained in detail.

In this study, six grid levels were used to model half the beam. With linear prolongation and sequential ordering, the multigrid algorithm yielded results which were of machine accuracy with work equivalent to 200 standard Gauss-Seidel iterations on the fine grid. Also with linear prolongation and sequential ordering, the V(1,n) cycle with n greater than 2 yielded better convergence rates than the V(n,1) cycle.

The restriction and prolongation operators were derived based on energy principles. Conserving energy during the inter-grid transfers required that the prolongation operator be the transpose of the restriction operator, and led to improved convergence rates. With energy-conserving prolongation and sequential ordering, the multigrid algorithm yielded results of machine accuracy with a work equivalent to 45 Gauss-Seidel iterations on the fine grid. The red-black ordering of relaxations yielded solutions of machine accuracy in a single V(1,1) cycle, which required work equivalent to about 4 iterations on the finest grid level.

17. Key Words (Suggested by Authors(s))	18. Distribution Statement
Geometric multigrid Finite elements Euler-Bernoulli beam Energy conserving prolongation red-black Gauss-Seidel	Unclassified - Unlimited Subject Category 39

19. Security Classif.(of this report)	20. Security Classif.(of this page)	21. No. of Pages	22. Price
Unclassified	Unclassified	59	A04

For sale by the National Technical Information Service, Springfield, Virginia 22161

NASA Langley Form 63 (June 1985)

Standard Bibliographic Page

1. Report No.	2. Government Accession No.	3. Recipient's Catalog No.
NASA TM-87761		

4. Title and Subtitle	5. Report Date
Multigrid Methods in Structural Mechanics	July 1986
	6. Performing Organization Code: 505-63-01

7. Author(s)	8. Performing Organization Report No.
I. S. Raju*, C. A. Bigelow, S. Ta'asan**, M. Y. Hussaini**	

9. Performing Organization Name and Address	10. Work Unit No.
NASA Langley Research Center Hampton, VA 23665-5225	11. Contract or Grant No.

12. Sponsoring Agency Name and Address	13. Type of Report and Period Covered
National Aeronautics and Space Administration Washington, DC 20546-0001	Technical Memorandum
	14. Sponsoring Agency Code

15. Supplementary Notes

*Analytical Services & Materials, Inc., work performed under NAS1-17808

**ICASE, NASA Langley Research Center, work performed under NAS1-17070

16. Abstract

Although the application of multigrid methods to the equations of elasticity has been suggested, few such applications have been reported in the literature. In the present work, multigrid techniques are applied to the finite element analysis of a simply supported Bernoulli-Euler beam, and various aspects of the multigrid algorithm are studied and explained in detail.

In this study, six grid levels were used to model half the beam. With linear prolongation and sequential ordering, the multigrid algorithm yielded results which were of machine accuracy with work equivalent to 200 standard Gauss-Seidel iterations on the fine grid. Also with linear prolongation and sequential ordering, the V(1,n) cycle with n greater than 2 yielded better convergence rates than the V(n,1) cycle.

The restriction and prolongation operators were derived based on energy principles. Conserving energy during the inter-grid transfers required that the prolongation operator be the transpose of the restriction operator, and led to improved convergence rates. With energy-conserving prolongation and sequential ordering, the multigrid algorithm yielded results of machine accuracy with a work equivalent to 45 Gauss-Seidel iterations on the fine grid. The red-black ordering of relaxations yielded solutions of machine accuracy in a single V(1,1) cycle, which required work equivalent to about 4 iterations on the finest grid level.

17. Key Words (Suggested by Authors(s))	18. Distribution Statement
Geometric multigrid Finite elements Euler-Bernoulli beam Energy conserving prolongation red-black Gauss-Seidel	Unclassified - Unlimited Subject Category 39

19. Security Classif.(of this report)	20. Security Classif.(of this page)	21. No. of Pages	22. Price
Unclassified	Unclassified	59	A04

For sale by the National Technical Information Service, Springfield, Virginia 22161